B.E. PROJECT

ON

PERFORMANCE ENHANCEMENT OF AN ACCELEROMETER USING INTELLIGENT TECHNIQUE

Submitted by

RAHUL AGGARWAL (477/IC/09)
RAVINDER KUMAR VERMA (480/IC/09)
SANJIT PALIWAL (492/IC/09)

(In partial fulfillment of B.E. (Instrumentation and Control Engineering) degree of University of Delhi

Under the Guidance of

Dr. K.P.S Rana and Dr. Vineet Kumar

DIVISION OF INSTRUMENTATION AND CONTROL ENGINEERING

NETAJI SUBHAS INSTITUTE OF TECHNOL0GY

UNIVERSITY OF DELHI, DELHI

JUNE 2013

ACKNOWLEDGEMENT

We, students of Netaji Subhas Institute of Technology, University of Delhi, currently studying in 4th year of B.E. program in Instrumentation and Control Engineering branch, are highly grateful to everyone who supported us in effectively completing our BTP titled 'PERFORMANCE ENHANCEMENT OF AN ACCELEROMETER USING INTELLIGENT TECHNIQUE'.

We are sincerely grateful to the Dr. K.P.S. Rana and Dr. Vineet kumar for providing us this opportunity to carry out our BTP at Instrumentation lab.

We would like to express a deep sense of gratitude and thanks profusely to them for their guidance and supervision. Without their wise counsel and able guidance, it would have been impossible to complete our work in this manner. Their guidance, help, ideas, insights and advise were instrumental in making this thesis possible. We are also thankful to them for all the resources they made available to us and for the time and resilience they spent to clear our doubts.

We will always remain indebted for their constant love, support, motivation and inspiration.

DECLARATION

This is to certify that the project entitled, "**Performance enhancement of an accelerometer using intelligent technique**" by **Rahul Aggarwal (477/IC/09)**, **Ravinder Kumar Verma (480/IC/09)** and **Sanjit Paliwal (492/IC/09)** is a record of bonafide work carried out by us, in the department of Instrumentation and Control Engineering, Netaji Subhas Institute of Technology, University of Delhi, New Delhi, in partial fulfillment of requirements for the award of the degree of Bachelor of Engineering in Instrumentation and Control Engineering, University of Delhi in the academic year **2012-2013**.

The results presented in this thesis have not been submitted to any other university in any form for the award of any other degree.

Rahul Aggarwal	Ravinder Kumar Verma	Sanjit Paliwal
477/IC/09	480/IC/09	492/IC/09

Instrumentation and Control Engineering Department
Netaji Subhas Institute of Technology (NSIT)
Azad Hind Fauj Marg
Sector-3, Dwarka, New Delhi
PIN - 110078

CERTIFICATE

This is to certify that the project entitled, ""**Performance enhancement of an accelerometer using intelligent technique**" by **Rahul Aggarwal (477/IC/09)**, **Ravinder Kumar Verma (480/IC/09)** and **Sanjit Paliwal (492/IC/09)**is a record of bonafide work carried out by them, in the department of Instrumentation and Control Engineering, Netaji Subhas Institute of Technology, University of Delhi, New Delhi, under our supervision and guidance in partial fulfillment of requirements for the award of the degree of Bachelor of Engineering in Instrumentation and Control Engineering, University of Delhi in the academic year **2012-2013**.

The results presented in this thesis have not been submitted to any other university in any form for the award of any other degree.

Dr. K.P.S. Rana
Associate Professor & Associate Head

Dr. Vineet Kumar
Sr. Lecturer

Instrumentation and Control Engineering Department
Netaji Subhas Institute of Technology (NSIT)
Azad Hind Fauj Marg
Sector-3, Dwarka, New Delhi
PIN - 110078

CERTIFICATE

This is to certify that the project entitled, "**Performance enhancement of an accelerometer using intelligent technique**" by **Rahul Aggarwal (477/IC/09)**, **Ravinder Kumar Verma (480/IC/09)** and **Sanjit Paliwal (492/IC/09)**is a record of bonafide work carried out by them, in the division of Instrumentation and Control Engineering, Netaji Subhas Institute of Technology, University of Delhi, New Delhi, in partial fulfillment of requirements for the award of the degree of Bachelor of Technology in Instrumentation and Control Engineering, University of Delhi in the academic year **2012-2013**.

Prof. A.P. Mittal
Head of the Department
Department of Instrumentation and Control Engineering
Netaji Subhas Institute of Technology (NSIT)
Azad Hind Fauj Marg
Sector-3, Dwarka, New Delhi
PIN - 110078

ABSTRACT

Accelerometer is a device used to measure static gravitational and dynamic accelerations and inertial velocity and position. We have limited our work for its application in measuring inertial acceleration only. First of all we have implemented a capacitive accelerometer in an open loop and showed the variation of parameters like displacement of proof mass and output voltage. After that we have closed its loop using PID controller and the results were better. We have tuned the PID using both Zeigler-Nichols and GA methods. Not much difference in the performance was observed. Finally, in order to further enhance its performance, we had used a Fuzzy PI + Fuzzy PD controller and tuned the fuzzy controller using GA techniques. And this implementation leads to increase its performance by 10 times in terms of ITAE value. As we told that we have confined our work only on capacitive accelerometers, but same can be implemented on other accelerometers such as tunneling accelerometer which has comparatively small size and higher sensitivity.

LIST OF TABLES

LIST OF FIGURES

LIST OF ABBREVIATIONS AND SYMBOLS

Symbol and Abbreviations	Definition
ε_0	Permitivity of air
ε_r	Permitivity of dielectric medium
μ	Viscosity of air
Δ	Change
Ω	Ohm
FLC	Fuzzy logic controller
GA	Genetic algorithm
ITAE	Integral of the time weighted absolute error
PI	Proportional integral
PD	Proportional derivative
PID	Proportional integral derivative
NL	Negative large
NS	Negative small
ZE	Zero
PS	Positive small
PL	Positive large
ZN	Ziegler-Nichols

INDEX OF EQUATIONS

TABLE OF CONTENTS

Chapter One: **INTRODUCTION TO ACCELEROMETERS**

1.1 Introduction

Accelerometers are defined as acceleration sensors that measure the linear acceleration along their sensitive axis. These devices have many application areas in the military and industrial fields, such as, activity monitoring in biomedical applications, active stabilization, robotics, vibration monitoring, navigation and guidance systems, and safety-arming in missiles. Until the introduction of microelectromechanical systems (MEMS), accelerometers were majorly utilized in the military applications, where cost is of little concern. With the advances in MEMS technology, micromachined accelerometers became the subject of extensive research and introduced to the cost sensitive commercial products. Being low cost, small size and having low power consumption, micromachined accelerometers are widely used for low-cost industrial applications, such as platform stabilization of video-cameras, shock monitoring of sensitive goods, electronic toys, robotics, and automotive applications. Automotive industry led the way to high volume applications of the micromachined accelerometers.

IC compatible micro fabrication processes enable the fabrication of these mechanical transducers together with their readout circuitry on the same substrate resulting in more reliable and higher performance accelerometers. There are severel companies manufacturing micromachined accelerometers in high-volumes. One of the most successful products in the market is the ADXL series of the Analog Devices. Analog Devices have a variety of surface micromachined accelerometers, monolithically fabricated with its readout circuitry. This company is capable of producing 2 million accelerometers per month and has fabricated its 100 millionth MEMS product recently. For each of these applications, different accelerometers with different performance requirements are employed. Although there are a number of accelerometers in the market for some of these applications, there is still need for the high performance accelerometers that can meet the expectations of high performance inertial measurement units for military applications.

1.2 Basic Operation Principle of Accelerometers

Operation of accelerometers depends on Newton's second law of motion, which states that any object undergoing acceleration is responding to a force. Newton's second law can be expressed with Equation 1.1, where F is the force exerted on the body, m is the mass of the body, and a is the acceleration of the body.

$$F = m * a \quad [1.1]$$

An accelerometer can be modeled by a mass-spring-damper system. Figure 1.1 shows the basic model of an accelerometer where seismic mass has a mass of m, suspension beams have an effective spring constant of k, and there is a damping factor of b. External acceleration displaces the seismic mass relative to the support frame. This displacement can be sensed with different transductions mechanisms.

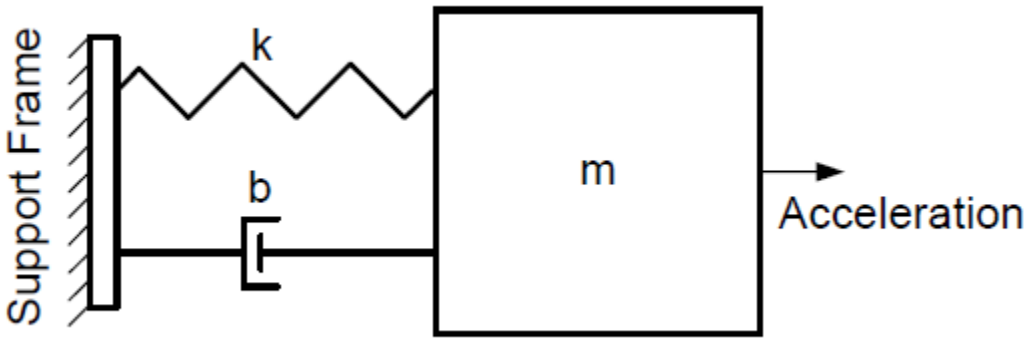

Figure 1.1: Basic model of an accelerometer

1.3 Various Types of Accelerometers

- Capacitive Accelerometer
- Tunneling Accelerometer
- Piezoresistive Accelerometer

- Piezoelectric Accelerometer

1.3.1 Capacitive Accelerometer

In capacitive accelerometers, displacement of the proof mass is measured capacitively. It provides a large output signal, good steady-state response, and better sensitivity due to low noise performance. The main drawback is that capacitive sensors are susceptible to electromagnetic fields from their surroundings; hence, they have to be shielded carefully. It is also unavoidable that parasitic capacitances at the input to the interface amplifiers will degrade the signal. Usually, a differential change in capacitance is detected.

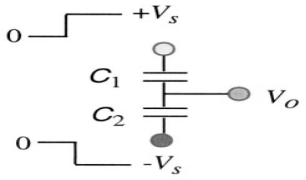

Figure 1.2: Differential type capacitive accelerometer.

As the proof mass moves away from an electrode, the capacitance decreases, and as it moves towards the electrodes, the capacitance increases. Neglecting fringe field effects, the change in capacitance is given by-

$$\Delta C = \varepsilon A\left(\frac{1}{d_0 - x} - \frac{1}{d_0 + x}\right) \qquad [1.2]$$

if $x^2 << d_0^2$, then

$$\Delta C = 2\varepsilon A \frac{x}{d_0^2} \qquad [1.3]$$

which is proportional to the deflection caused by the input acceleration only if the assumption of small deflections is made. For precision accelerometers this assumption may be not justifiable, and hence, closed loop control can be used to keep the proof mass deflections small.

1.3.2 Tunneling Accelerometer

The most sensitive method for measuring position is to exploit the exponential dependence of current on the distance between an atomically sharp tunneling tip and an electrode.

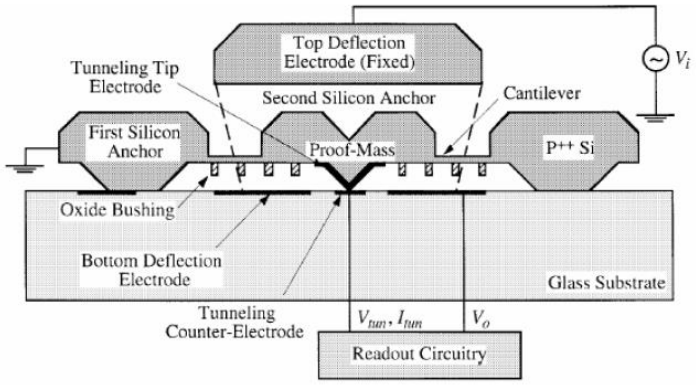

Figure 1.3: Tunneling current accelerometer.

As shown in figure a sharp conducting tip near a flat electrode. When the distance between the tip and the electrode approaches nanometer dimensions, a conducting path is created by direct tunneling of electrons across the gap.

If a bias voltage V_B is applied between the electrodes, a tunneling current I_t flows. The dependence of I_t on the gap d_t is of the form:

$$I = I_o \exp(-\beta\sqrt{\phi z}) \qquad [1.4]$$

where I_0 is a scaling current dependent on material and tip shape (a typical value is 1.4×10^{-6}A), β is a conversion factor with a typical value of 10.25 $eV^{-1/2}$/nm, ϕ is the tunnel barrier height with a typical value of 0.5 eV, and z is the tip/electrode distance. A distance change of only 0.01 nm results in a 4.5% change in tunnel current, and changes well below this level can be measured. However, because of the strong exponential dependence of current on distance, it is necessary to use force feedback with these tips to keep the distance and corresponding current within a useful operating range. Electrostatic force-feedback is employed for the majority of research devices and this keeps the separation distance approximately constant. The acceleration can then be inferred from the voltage required to produce the necessary electrostatic force.

The proof mass deflection electrode is used to pull the proof mass, by the electrostatic force, into close proximity so that a tunneling current begins to flow. The cantilever deflection electrode is used for closed loop control to maintain the distance

between the tip and the cantilever constant. Theoretically, this is the most sensitive detection mechanism.

1.3.3 Piezoresistive Accelerometer

These devices tended to use a piezoresistive position measurement interface, as these are easy to fabricate in silicon and the read-out circuit is relatively simple; they provide a low-impedance output signal and a conventional resistive bridge circuit can be used. Furthermore, early piezoresistive accelerometers were directly based on the expertise gained through the development of micro machined pressure sensors. A serious drawback, however, is that the output signal tends to have a strong temperature dependency because the piezoresistors inherently produce thermal noise and the output signal is relatively small. Typical performance figures for these devices show a sensitivity of 1 - 3 mV/g, 5g - 50g dynamic range, and an uncompensated temperature coefficient of 0.2% per degree C.

They typically consist of a multi-wafer assembly with the central wafer comprising the bulk-micro machined proof mass and suspension system and either silicon or Pyrex glass wafers on top and bottom to provide over-range protection and near critical damping due to squeeze film effects. The cross-sectional view of Piezo-resistive accelerometer is shown in the Figure 1.4.

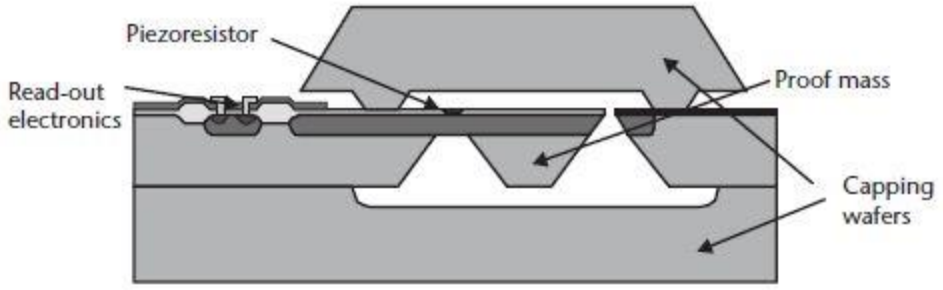

Figure 1.4: Cross-sectional view of the piezoresistive accelerometer

The sensing element is encapsulated by top and bottom wafers, which are bonded to the middle layer at wafer level. Small air gaps were formed into the cap-wafers by dry-etching in order to provide near-critical damping.

The disadvantages of piezoresistive signal pick-off can be partially overcome by integrating the read-out electronics on the same chip.

1.3.4 Piezoelectric Accelerometer

Macroscopic accelerometers quite commonly use piezoelectric materials for the detection of the proof mass. There has been a range of micromachined accelerometers reported that are based on this principle. The advantage is the higher bandwidth of these sensors, which can easily reach several tens of kilohertz. The major drawback, however, is that they do not respond to static and low-frequency acceleration signals because of unavoidable charge leakage.

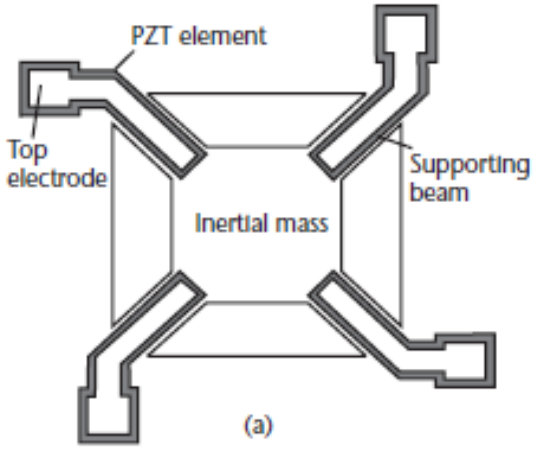

Figure 1.5: Design of a piezoelectric accelerometer using thick-film printed PZT.

The fabrication process is simple and the yield was shown to be very high. The sensitivity was given as 16 pC/ms^{-2}, which was considerably higher than the devices using thin, sputtered zinc oxide (ZnO) layers.

1.4 Objective of the study and thesis organization

1.4.1 Objectives

A capacitive accelerometer has been modelled and simulated in previous works of Grigorie [4]. The linear range of the open loop accelerometer and closed loop accelerometer with PID controller tuned using Ziegler-Nichols is ±4g and ±20 g respectively in the work of Grigorie. Objective of this thesis is to model and simulate a capacitive accelerometer system having a high linear range, high sensitivity and low

ITAE value that improvement on the work done by Grigorie. We have in thesis designed and simulated closed loop accelerometer with PID controller tuned using GA and closed loop accelerometer with Fuzzy PI + Fuzzy PD controller tuned using GA with linear range of ±30g and ±50 g respectively. NI LabVIEW software was used for simulation of the accelerometer.

1.4.2 Thesis Organisation

The organisation of the thesis is as follows:

Chapter 2 In this chapter modelling and simulation of the open loop accelerometer is done.

Chapter 3 In this chapter designing and simulation of the closed loop accelerometer with PID controller tuned using Ziegler Nichols and closed loop accelerometer with PID controller tuned using GA is done.

Chapter 4 In this chapter designing and simulation of the closed loop accelerometer with Fuzzy PI + Fuzzy PD controller tuned using GA is done.

Chapter 5 In this chapter comparative study of the different configurations of the capacitive accelerometer are done on the parameters of displacement of proof mass, ITAE value and output voltage of accelerometer and also scope for future work is given.

***

Chapter Two: **ACCELEROMETER MODEL & OPEN LOOP PERFORMANCE**

2.1 Introduction

The accelerometer provides a measure of acceleration in form of an electrical output signal. One reason this sensor is of special significance is the fact that by integrating the output signal, an accelerometer can also provide a measure of velocity and position.

In open loop arrangement of capacitive type accelerometer there are two electrodes, placed on opposed sides of the mobile plaque. The couple of fixed electrodes and the mobile plaque form two capacitors whose capacities vary with the application of an acceleration that has the ability to change the proof mass position.

2.2 Derivation of the Motion Equation

The measurement of acceleration always relies on classical Newton's mechanics. Normally the acceleration to which a body is subjected is of interest; the accelerometer being rigidly attached to that body.

The physical quantities from Figure 2.1 are: m - proof mass, $\vec{a}$,y - acceleration and position of the carrying vehicle , $\vec{a}_x$, x - acceleration and proof mass position with respect

to the carrying vehicle. $\vec{F}_e, \vec{F}_a, \vec{F}_i$ – the elastic, the damping and the inertial force respectively. The absolute values of the three forces are provided by the following equations:

$$\vec{F}_e = kx \qquad [2.1]$$

$$\vec{F}_a = b\frac{dx}{dt} \qquad [2.2]$$

$$\vec{F}_i = ma = m\frac{d^2x}{dt^2} \qquad [2.3]$$

where k is the resulting elasticity constant and b is the viscous damping coefficient

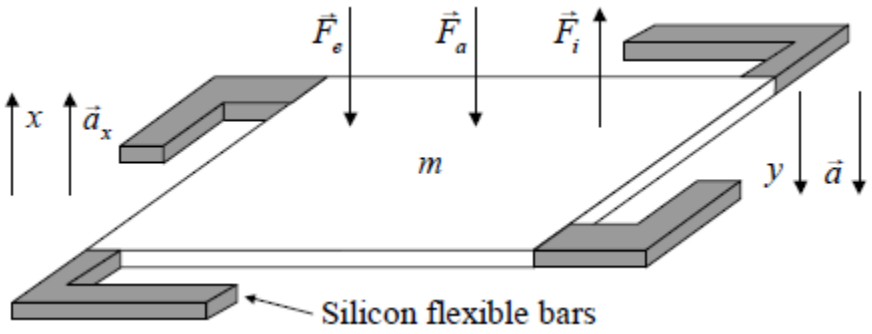

Figure 2.1: Mechanical sensing element.

When the fixed electrodes are not supplied by electric energy, according to fig. 1.1 the motion equation of the proof mass is

$$m\frac{d^2y}{dt^2} = m\frac{d^2x}{dt^2} + b\frac{dx}{dt} + kx \qquad [2.4]$$

The accelerometer is miniaturized, so the viscous damping is provided by the air that is enclosed in its watertight carcass. For relatively large displacements of the mobile plaque (as high as μm) the viscous amortization is given by the expression

$$b(x) = \frac{1}{2}\mu A^2\left[\frac{1}{(d_0 - x)^3} + \frac{1}{(d_0 + x)^3}\right] \qquad [2.5]$$

where μ is the air viscosity, A is the mobile plaque area and $2d_0$is the distance between the fixed electrodes.

If the fixed electrodes are supplied by the voltages

$$v_1 = V_1 \sin \omega t \qquad [2.6]$$

$$v_2 = -v_1 = V_1 \sin \omega t \qquad [2.7]$$

then the following electrostatic forces will act over the mobile plaque (fig 2.2)

$$F_{el1} = \frac{\varepsilon_0 A}{2}\frac{v_1^2}{(d_0 - x)^2} = \frac{\varepsilon_0 A}{4}\frac{V_1^2}{(d_0 - x)^2}(1 - \cos 2\omega t) \qquad [2.8]$$

$$F_{el2} = \frac{\varepsilon_0 A}{2}\frac{v_1^2}{(d_0 + x)^2} = \frac{\varepsilon_0 A}{4}\frac{V_1^2}{(d_0 + x)^2}(1 - \cos 2\omega t) \qquad [2.9]$$

The frequency of supplying voltage is very high ($f = 10^5 Hz$).

The sensitive element behaves like low pass mechanical filter so the expressions are:

$$F_{el1} = \frac{\varepsilon_0 A}{4}\frac{V_1^2}{(d_0 - x)^2} \qquad [2.10]$$

$$F_{el2} = \frac{\varepsilon_0 A}{4}\frac{V_1^2}{(d_0 + x)^2} \qquad [2.11]$$

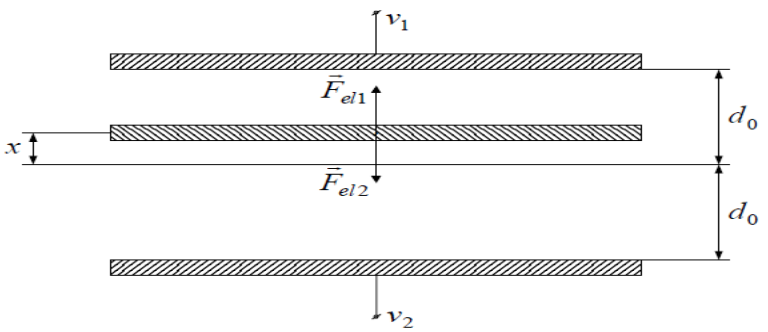

Figure 2.2: Action of electrostatic forces

The resulting force will be

$$F_{el} = F_{el1} - F_{el2} = \frac{\varepsilon_0 A V_1^2}{4}\left[\frac{1}{(d_0 - x)^2} - \frac{1}{(d_0 + x)^2}\right] \qquad [2.12]$$

The motion equation becomes

$$m\frac{d^2y}{dt^2} = m\frac{d^2x}{dt^2} + b\frac{dx}{dt} + kx - F_{el} \qquad [2.13]$$

Using [2.5] and [2.12], the equation [2.13] becomes

$$\frac{d^2x}{dt^2} = a - \frac{\mu A^2}{2m}\left[\frac{1}{(d_0-x)^3} + \frac{1}{(d_0+x)^3}\right]\frac{dx}{dt} - \frac{k}{m}x + \frac{\varepsilon_0 A V_1^2}{4}\left[\frac{1}{(d_0-x)^2} - \frac{1}{(d_0+x)^2}\right] \qquad [2.14]$$

2.3 Signal Pick-off

The measurement of the position of the seismic mass in a capacitive sensing element is commonly realized by applying a high-frequency (100 kHz in this case) sinusoidal signal to the top electrode 'v_1', and the same signal in antiphase to the bottom

electrode 'v_2' as explained in above section The signal coupled through to the seismic mass is passed to a charge amplifier. Figure 2.4 shows the pick-off circuit arrangement

The seismic mass acts as the common electrode for the two capacitors in series, $C_1$and C_2(Figure 2.3).

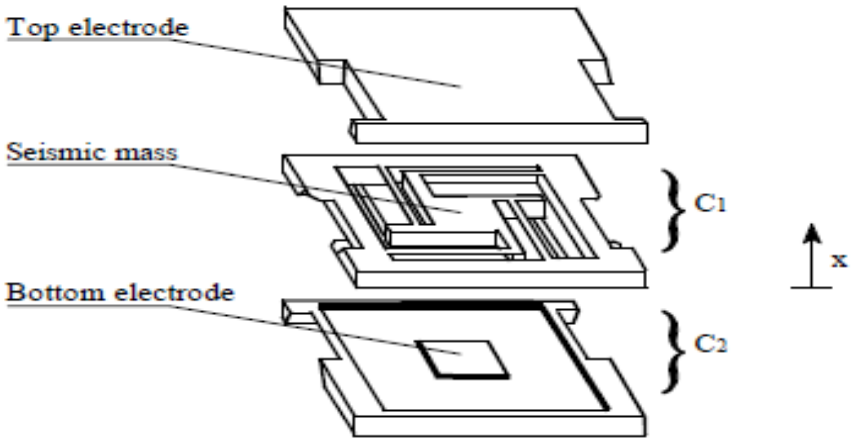

Figure 2.3: Sensing element.

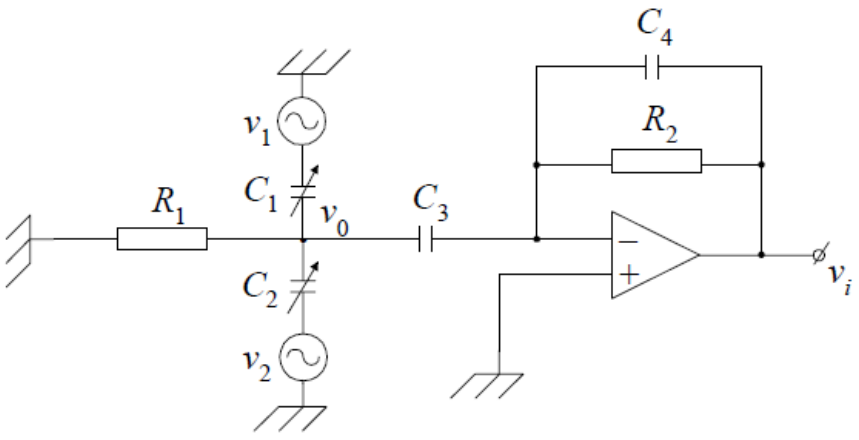

Figure 2.4: Charge amplifier circuit for measuring the imbalance in capacitance.

C_1 *and* C_2 represent the variable capacitors of the sensing element, C_3 is required to block any d.c. Signal that may be present at the seismic mass (the centre point between

the capacitors) and could cause the operational amplifier to saturate R_1 keeps the seismic mass at a defined potential and has to be sufficiently large, the time constant $\tau = C_{1/2}R_1$should be at least ten times bigger than the time period of the excitation signal, thus R_1 > 10 $M\Omega$. In this design R_1 was chosen to be 250 MΩ.

C_1 and C_2 are given by the equation:

$$C_1 = \frac{\varepsilon_0 \varepsilon_r A}{(d_0 - x)} = \frac{\varepsilon_0 \varepsilon_r A d_0}{d_0^2 - x^2} + \frac{\varepsilon_0 \varepsilon_r A x}{d_0^2 - x^2} \quad [2.15]$$

$$C_2 = \frac{\varepsilon_0 \varepsilon_r A}{(d_0 + x)} = \frac{\varepsilon_0 \varepsilon_r A d_0}{d_0^2 - x^2} - \frac{\varepsilon_0 \varepsilon_r A x}{d_0^2 - x^2} \quad [2.16]$$

$If\ x \ll d_0\ , one\ can\ consider\ the\ approximation$

$$C_1 \cong C_0 + \Delta C\ \&\ C_2 \cong C_0 - \Delta C \quad [2.17]$$

where $C_0 = \frac{\varepsilon_0 \varepsilon_r A}{d_0}$

& $\Delta C = \frac{\varepsilon_0 \varepsilon_r A x}{d_0^2 - x^2}$

The proof mass potential V_0 can be calculated using the equation:

$$V_0(s) = \frac{V_1(s) s C_1 + V_2(s) s C_2}{s(C_1 + C_2 + C_3) + 1/R_1} \quad [2.18]$$

$$V_i(s) = -V_0(s) \frac{s C_3 R_2}{1 + s C_4 R_2} \quad [2.19]$$

$$V_i(s) = \frac{2 s^2 C_3 R_2 \Delta C V_1(s)}{(1 + s C_4 R_2)[s(2C_0 + C_3) + 1/R_1]} \quad [2.20]$$

2.4 Demodulation Circuit Design and Model

In order to preserve the information of the sign of the seismic mass deflection and to cancel resistive terms it is necessary to phase-sensitively demodulate the output voltage of the charge amplifier and pass it through a low-pass filter. This is achieved by the arrangement shown in Figure 2.5:

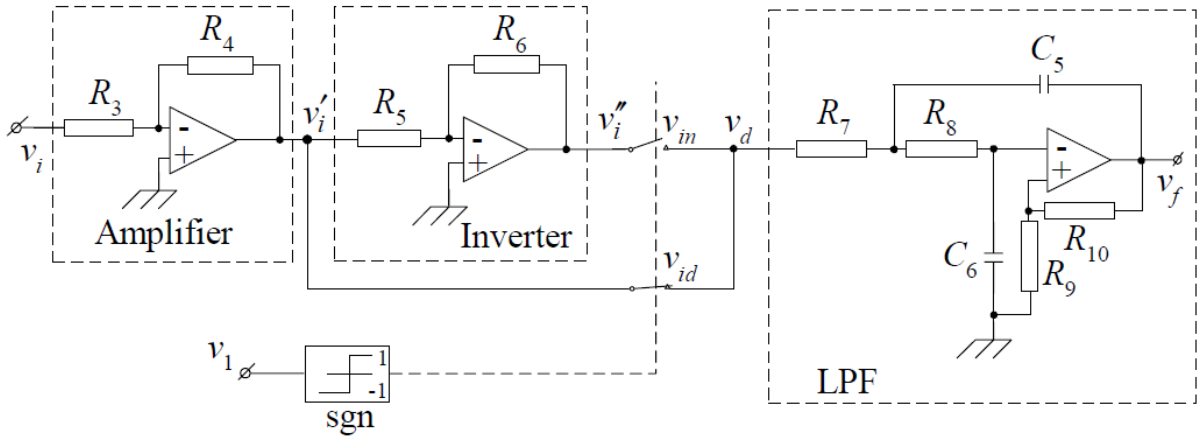

Figure 2.5: Phase-sensitive demodulation.

The excitation voltage ‘v1', is used to derive a logic signal which controls two analogue switches. The output voltage of the operational amplifier is first buffered and together with its inverted signal subjected to the analogue switches from which the output voltage is then filtered by a second order low-pass.

The demodulator electronic scheme can be modelled as depicted by Figure 2.5. The transfer functions of the three blocks from Figure 2.5 are

$$\frac{V_i'(s)}{V_i(s)} = -\frac{R_4}{R_3} \qquad [2.21]$$

$$\frac{V_i''(s)}{V_i'(s)} = -\frac{R_4}{R_3} \quad [2.22]$$

$$\frac{V_f(s)}{V_d(s)} = \frac{R_9 + R_{10}}{s^2 R_7 R_8 R_9 C_5 C_6 + s[C_6 R_9 (R_7 + R_8) - C_5 R_7 R_{10}] + R_9} \quad [2.23]$$

The following notation are used:

$$k_a = -\frac{R_4}{R_3}$$

$$k_A = 1 + \frac{R_{10}}{R_9}$$

$$a_2 = R_7 R_8 R_9 C_5 C_6$$

$$a_1 = C_6(R_7 + R_8) - \frac{C_5 R_7 R_{10}}{R_9}$$

The equations become

$$\frac{V_i'(s)}{V_i(s)} = k_a \quad [2.24]$$

$$\frac{V_i''(s)}{V_i'(s)} = -1 \quad [2.25]$$

$$\frac{V_f(s)}{V_d(s)} = \frac{k_A}{a_2 s^2 + a_1 s + 1} \quad [2.26]$$

2.5 Mathematical Model for the Open Loop Accelerometer

With the above considerations it was now possible to derive a mathematical model for the open loop accelerometer, Figure 2.6.

This model is a true mechatronic system consisting of a mechanical component, the micro machined sensing element and an electronic part, the pick-off and demodulation circuitry. From the deflection of the seismic mass ‘x’ the instantaneous values of C1 and C2 are calculated; The pick-off circuit measures the imbalance in capacitance which is converted into an output signal by the demodulation circuit and the low pass filter.

Included in the model are the electrostatic forces on the seismic mass generated by the excitation voltages. As the electrostatic forces depend on the voltage and the position of the seismic mass, The function blocks calculating the forces have two input variables.

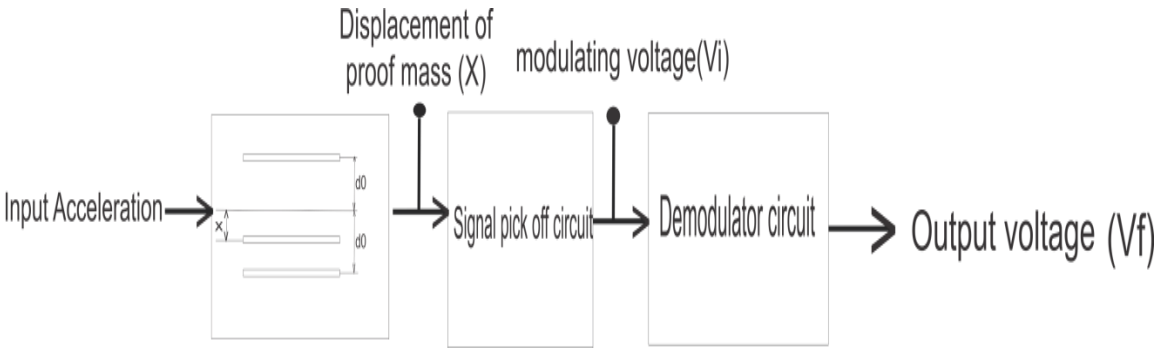

Figure 2.6: Block Diagram of Open loop accelerometer

Table 2.1: Parameter values.

Parameter	Value	Parameter	Value
m	8.2 mg	k_A	1.56
A	12 mm^2	a_1	$0.3888*10^{-3}s$
d_0	10um	a_2	$72.9*10^{-9}s^2$
ε_r	1	K_a	-10
k	88.3 N/m	C_0	10.6pF
μ	$1.8 *10^{-5}$	R_3	1kΩ
f	100KHz	$R_4=R_5=R_6=R_9$	10kΩ
C_3	1nF	$R_7=R_8$	180kΩ
C_4	22nF	R_{10}	5.6kΩ
$C_5=C_6$	1.5nF		

2.6 Results

The displacement of the proof mass, change in capacitance, output voltage of the accelerometer for different step like input acceleration signals are presented in Figure 2.7, Figure 2.8 and Figure 2.9 respectively. The displacement of the proof mass for different sine input acceleration signals are presented in Figure 2.10.

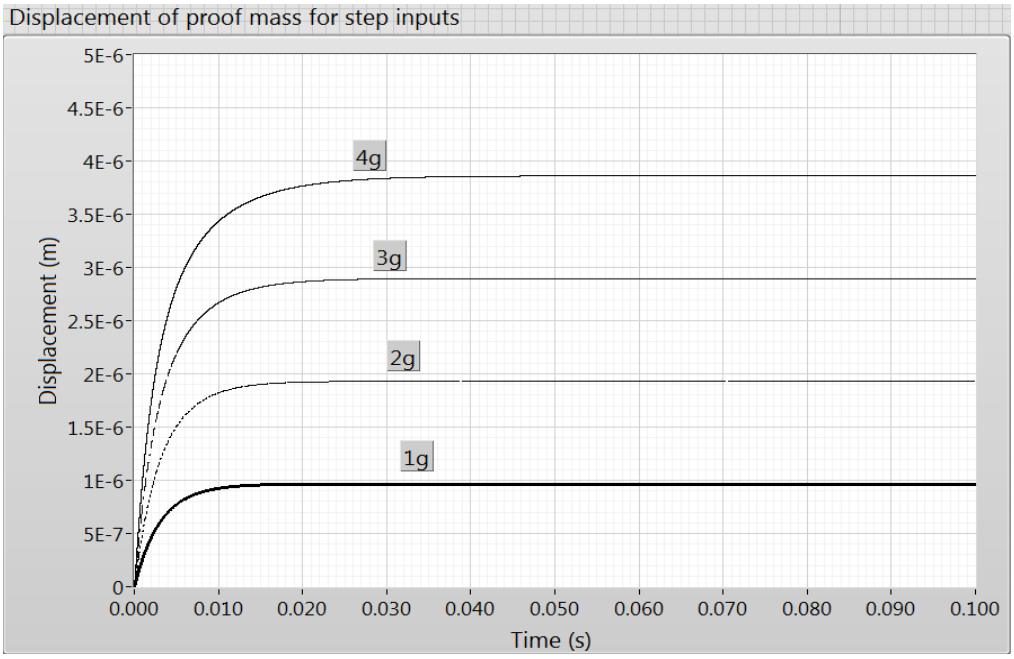

Figure 2.7: Displacement of proof mass.

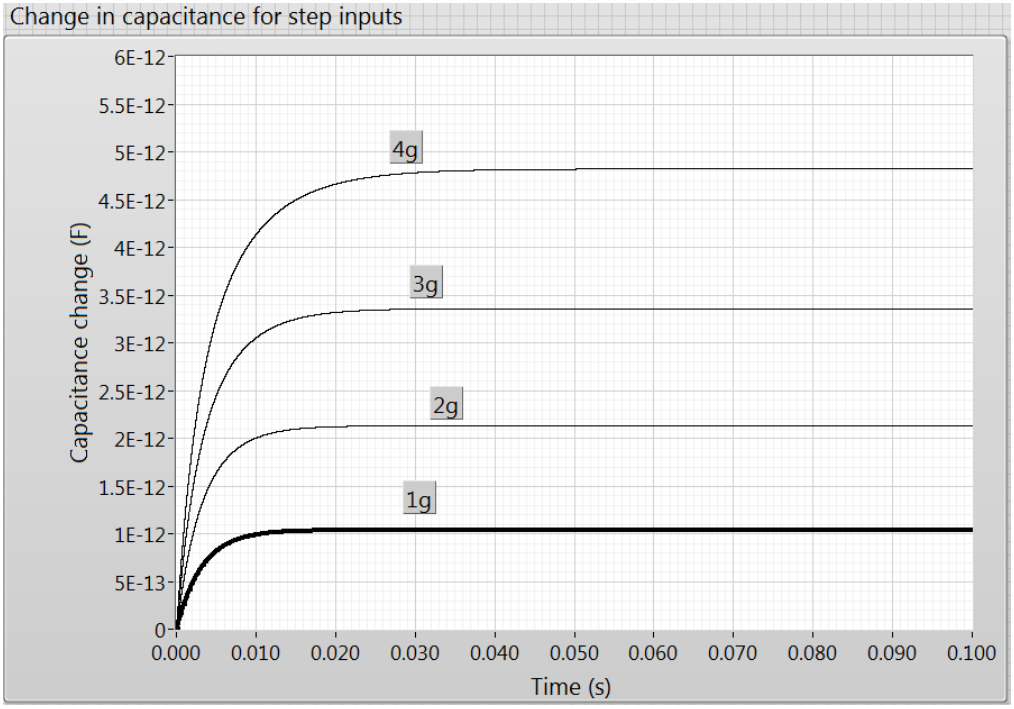

Figure 2.8: Change in capacitance vs time.

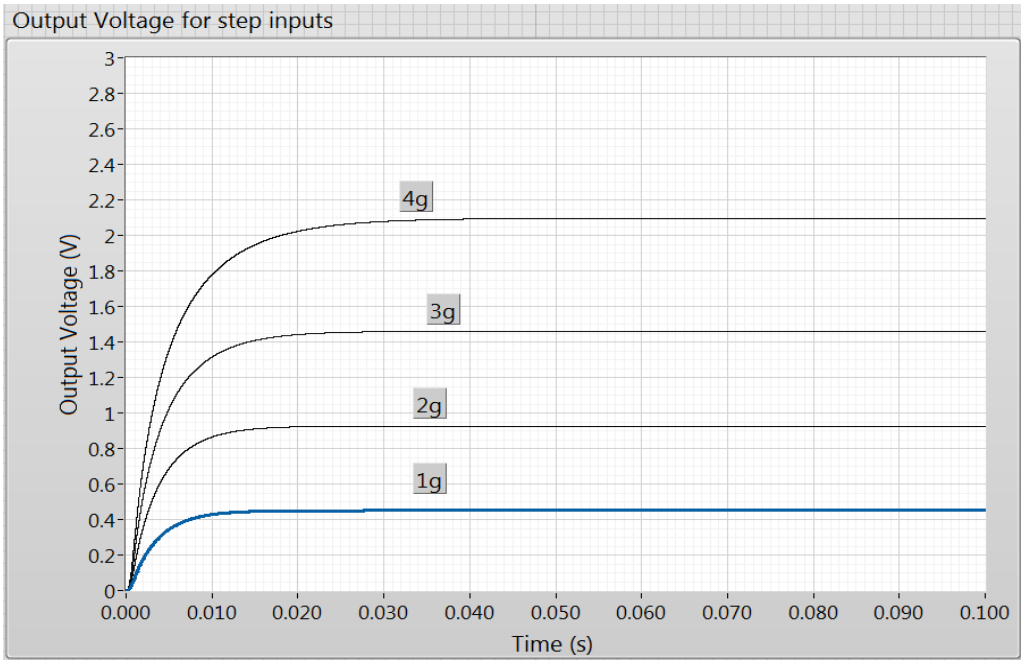

Figure 2.9: Output voltage of open loop accelerometer

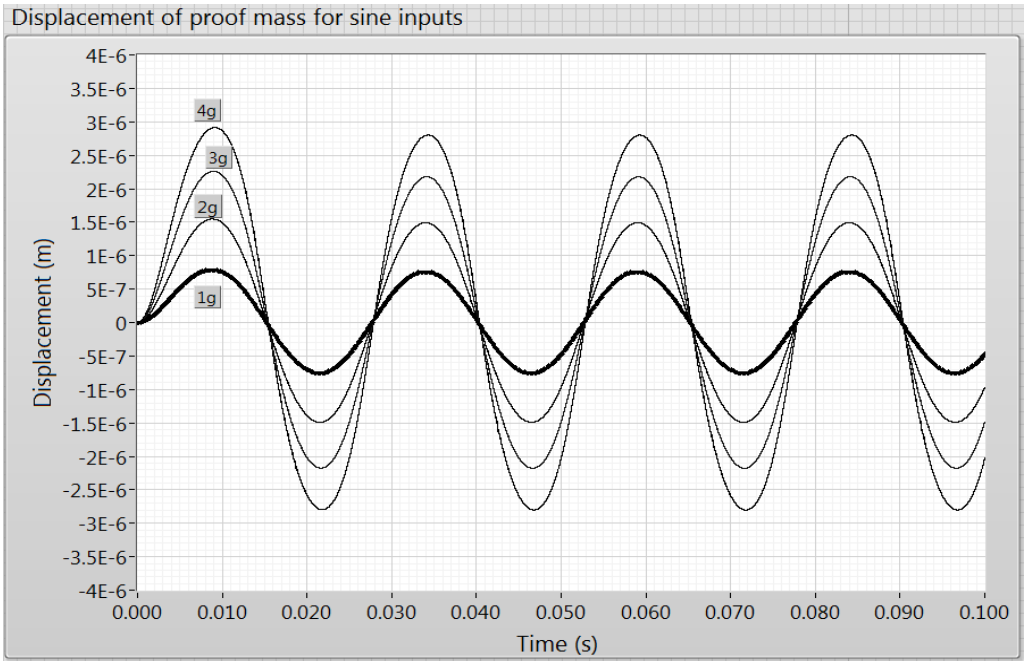

Figure 2.10: Displacement of proof mass for sine input

***

Chapter Three: **PERFORMANCE ENHANCEMENT OF ACCELEROMETER USING PID CONTROLLER**

3.1 Introduction

The open loop accelerometer has limited performance in terms of bandwidth, linearity and dynamic range. Additionally, nonlinear effects caused by, the damping and the electrostatic forces required for the signal pick-off, increase with the deflection of the seismic mass. One method of reducing these nonlinearities and improving the performance is to use the sensing element in a closed loop control system in which a reaction force is applied to the seismic mass to keep it at the central position between the electrodes. Owing to the small distances between the fixed electrodes and the proof mass, for the miniaturized accelerometers, an electrostatic force was chosen as reaction force. The controller used is PID controller and tuning is made using the minimum error surface criteria Ziegler-Nichols.

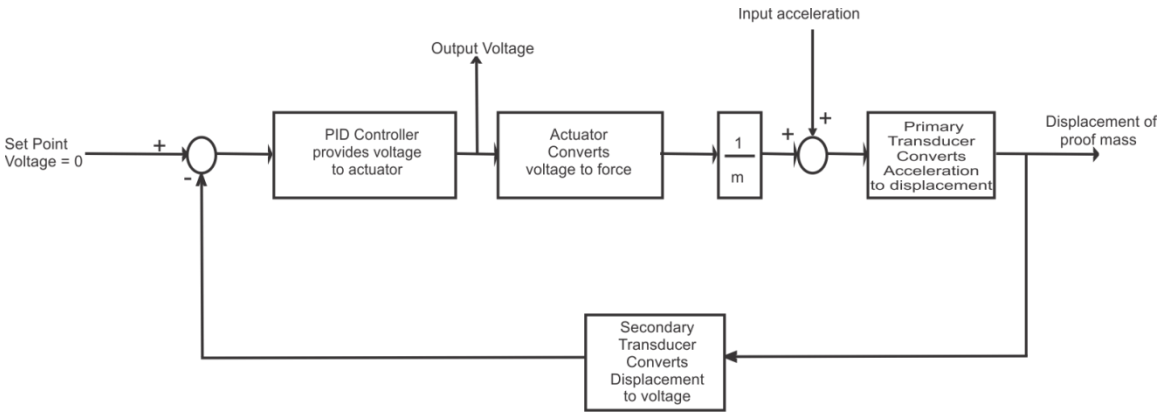

Figure 3.1: Accelerometer with PID Controller in closed loop

3.2 Electrostatic Feedback Force

Electrostatic forces are only of attraction type, it is difficult to maintain a negative reaction. The most popular situation in this case is the superposition of two electrostatic forces that should act over the proof mass. Thus the resulting force provides a negative reaction. A supplementary problem comes from the fact that the negative reaction is a nonlinear function owing to the dependency of the electrostatic force with the voltage square and on the reversed value of the distance between the electrodes. Moreover, because the accelerometer has only 3 connecting points (2 fixed electrodes and the proof mass), one must prevent a possible interaction between the reaction signals and those of excitation, required by the demodulating circuit. For the studied accelerometer, the condition is fulfilled because one uses a phase-sensitive demodulating circuit, controlled by a high-frequency signal (f = 100 kHz).

In order to obtain a corresponding reaction force along the fixed electrodes, one must apply a biasing voltage V_B, but with a different sign. In the same time, on both electrodes on apply the reaction voltage v_r, so as on each electrode 3 voltage signals will be superposed.

$$v_s = v_1 - V_B + v_r \qquad [3.1]$$

$$v_i = v_2 + V_B + v_r \qquad [3.2]$$

where v_s , v_i are the voltages applied on the high and low electrode respectively . The electrostatic forces existing between the fixed electrodes and the proof mass can be described as follows:

$$F_{el1} = \frac{1}{2}\varepsilon_0 A \frac{{v_s}^2}{(d_0 - x)^2} = \frac{1}{2}\varepsilon_0 A \frac{(v_1 - V_B + v_r)^2}{(d_0 - x)^2} \quad [3.3]$$

$$F_{el2} = \frac{1}{2}\varepsilon_0 A \frac{{v_i}^2}{(d_0 + x)^2} = \frac{1}{2}\varepsilon_0 A \frac{(v_2 + V_B + v_r)^2}{(d_0 + x)^2} \quad [3.4]$$

So, the resulting electrostatic force can by calculated with the relation

$$F_{elr} = F_{el1} - F_{el2} = \frac{1}{2}\varepsilon_0 A \left[\frac{(V_1 \sin(\omega t) - V_B + v_r)^2}{(d_0 - x)^2} - \frac{(-V_1 \sin(\omega t) + V_B + v_r)^2}{(d_0 + x)^2}\right] \quad [3.5]$$

considering $x^2 \ll {d_0}^2$,

$$F_{elr} = \frac{2\,\varepsilon_0 A}{{d_0}^4}\left[x({V_1}^2 \sin^2(\omega t) + {V_B}^2 + {v_r}^2 - 2V_1 V_2 \sin(\omega t)) - d_0 v_r (V_1 \sin(\omega t) - V_B)\right] \quad [3.6]$$

For an ideal closed loop the proof mass is close by the position $x = 0$, therefore is considered as valid for the approximation

$$F_{el} \cong \lim_{x \to 0} \frac{2\,\varepsilon_0 A}{{d_0}^3}\left[x\left(\frac{{V_1}^2}{2} + {V_B}^2 + {v_r}^2\right) - d_0 v_r V_B\right] = -\frac{2\,\varepsilon_0 A V_B}{{d_0}^2} v_r \quad [3.7]$$

Thus, one observe that if the proof mass displacements are very small than the resulting electrostatic force is a linear function of feedback voltage.

3.3 Genetic Algorithms

Genetic algorithms are stochastic search methods that can be used to search for an optimal solution to the evolution function of an optimization problem. Holland proposed GAs in the early seventies as computer programs that mimic the natural evolutionary process. De Jong extended GAs to functional optimization and a detailed mathematical model of a GA was presented by Goldberg.

GAs differ from classical optimization and search methods in several respects. Rather than focusing on a single solution, GAs operate on group of trial solutions in parallel where they manipulate a population of individuals in each generation (iteration) where each individual, termed as the chromosome, represents one candidate solution to the problem. Within the population, individuals survive to reproduce and their genetic materials are recombined to produce new individuals as offspring's. The genetic material is modeled by some finite-length data structures.

As in nature, selection provides the necessary driving mechanism for better solutions to survive. Each solution is associated with a fitness value that reflects how good it is compared with other solutions in the population. The recombination process is simulated through a crossover mechanism that exchanges portions of data strings between chromosomes. New genetic material is also introduced through mutation that causes random alterations of the strings. The frequency of occurrence of these genetic operations is controlled by certain pre-set probabilities. The selection, crossover, and mutation processes constitute the basic GA cycle or generation, which is repeated until some pre-

determined criteria are satisfied. Through this process, successively better and better individuals of the species are generated.

In a nutshell, a GA entails four fundamental steps as follows:

Step 1: Create an initial population of random solutions (chromosomes) by some means.

Step 2: Assess the chromosomes for fitness using the criteria imposed on the required solution and create an elite set of chromosomes by selecting a number of chromosomes that best satisfy the requirements imposed on the solution.

Step 3: If the top-ranking chromosome in the elite set satisfies fully the requirements imposed on the solution, output that chromosome as the required solution, and stop. Otherwise, continue to Step 4.

Step 4: Apply crossover between pairs of chromosomes in the elite set to generate more chromosomes and subject certain chromosomes chosen at random to mutations, and repeat from Step 2.

A schematic representation of the genetic search approach is presented in Figure 3.2.

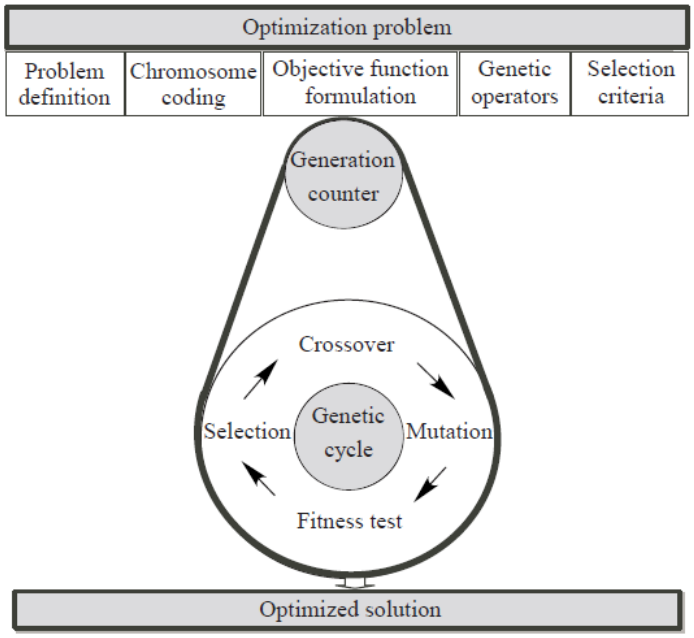

Figure 3.2: Conceptual representation of the optimization process through a genetic algorithm.

3.4 PID Control

PID or three-term controllers are widely used in industry. The PID name comprises the first letters of the three terms which make up this controller:

1. P stands for the Proportional term in the controller
2. I stands for the Integral term in the controller
3. D stands for the Derivative term in the controller

The Laplace transform formalism had begun to be understood and used by engineers to study the performance of op-amps and hence the performance of PID control. These simple Laplace transform links, like [1/s] to represent an Integrator and [s] to represent a Differentiator, helped to establish a theoretical basis for analysing a PID

control design. Figure 3.3 shows the three links for the PID controller. Figure shows the PID blocks, (b) shows the time function forms of the blocks and finally (c) shows the Laplace function forms of the blocks.

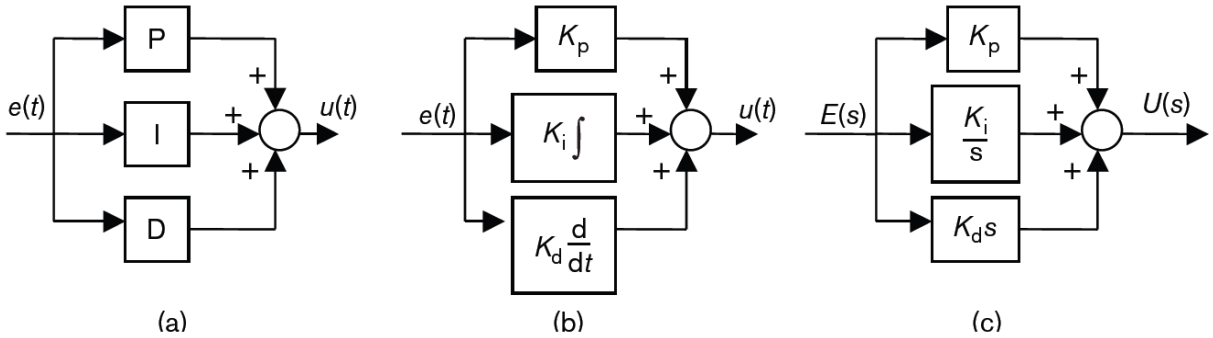

Figure 3.3: PID controller blocks.

3.4.1 Proportional Action

Increasing the proportional action:

- means increasing the numerical value of the proportional gain, Kp
- speeds up the transient portion of the reference tracking response and the transient portion of the load disturbance response
- decreases but does not entirely remove or eliminate the output offset from the desired reference value
- decreases but does not entirely eliminate the offset in the output due to the constant load disturbance
- generally increases the size of the control signal which achieves good reference tracking and disturbance rejection in the system output

- may cause the controller signal to be too large which may lead to saturation or limiting problems with the system actuators

3.4.2 Integral Action

Introducing integral action into a controller means incorporating an integral term [Ki/s] into the controller.

- Increasing the amount of integral action in a controller means that the integral gain Ki has an increasing numerical value.
- The presence of integral action in a controller usually leads to a wider range of closed-loop system responses.
- Selecting a value for integral gain Ki shapes the dynamics of both reference tracking and disturbance rejection responses.
- The presence of integral action in a controller eliminates constant offset signals in steady state for both reference tracking and disturbance rejection responses. This property is guaranteed and does not depend on using prior process gain modeling information.

3.4.3 Derivative Action

Introducing derivative action into the controller means incorporating a derivative term into the controller.

- Increasing the amount of derivative action means that the numerical value of the derivative
- Derivative action is usually associated with the controller anticipating the future direction of error signals.
- The damping ratio of the closed-loop system response can be tuned by changing the amount of derivative gain in the controller. This is an important practical property of derivative control.
- Derivative control will affect the shape of both the reference tracking and disturbance rejection responses.
- Derivative control has no effect on constant offsets in either the reference tracking or disturbance rejection responses. This is because the derivative of a constant error is zero and so the controller does not respond to the presence of the constant error. This is quite the opposite effect of the use of integral control.

3.4.4 PID Tuning- Ziegler Nichols

Ziegler Nichols tuning method is as follows:

- one considers the regulator as a proportional one and it is tuned with respect to the $K_P$parameter;
- one increases the amplification factor K_P until the response of the automatic system will be self-sustained oscillatory. One memorizes the value $K_{P0}$of $K_P$for

which the system has an oscillatory behaviour and the value of oscillations semi-period T_0.

The optimal values for the parameters of the PID controller are determined using the relations

$$K_P = 0.45\, K_{P0} \quad [3.8]$$

$$T_I = 0.85\, T_0 \quad [3.9]$$

$$K_I = \frac{K_p}{T_I} \quad [3.10]$$

$$T_D = 0.12\, T_0 \quad [3.11]$$

$$K_I = K_p T_D \quad [3.12]$$

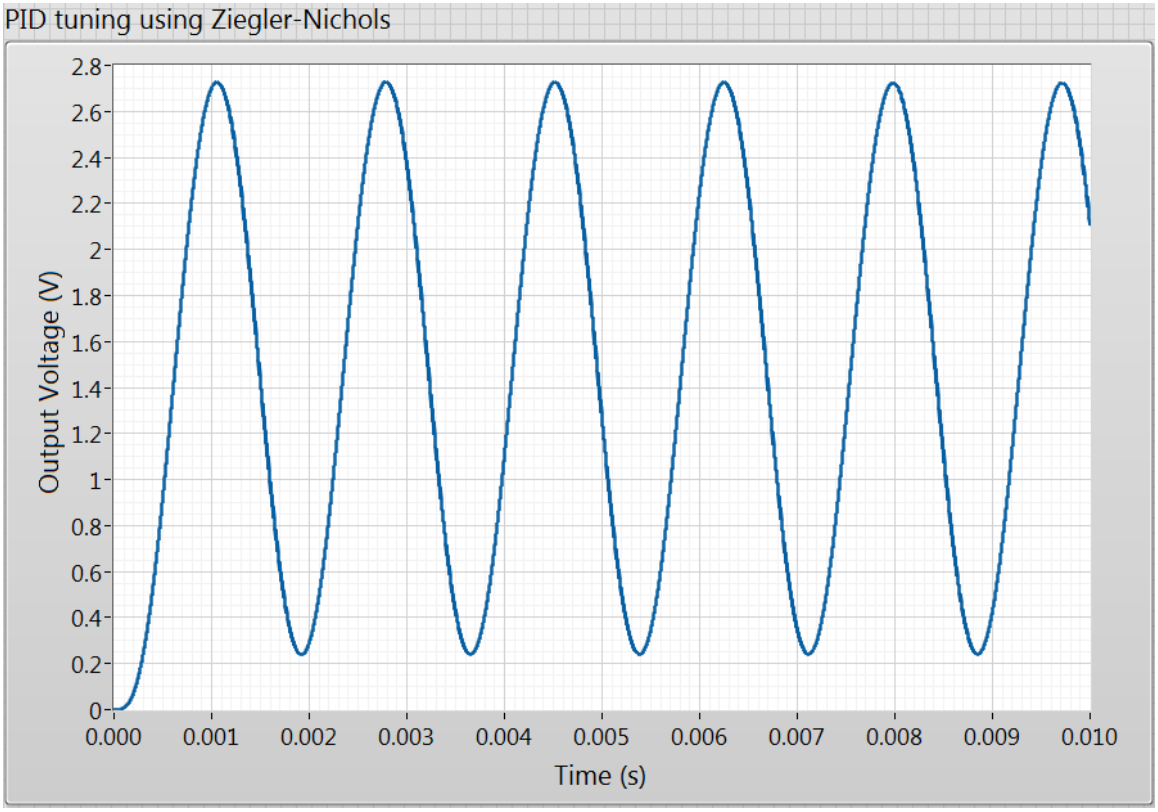

Figure 3.4: PID Tuning using Ziegler- Nichols.

From the simulation of the schema one observe that the system has an oscillatory behaviour starting with $K_{P0} \cong -50$ and $T_0 \cong 2 \cdot 10^{-3} s$ as shown in Figure 3.4. From Equations [3.8] to [3.12] we get,

$K_P = 22, K_I = 13200\ s^{-1}\ and\ K_D = 5.28 \cdot 10^{-3} s$

3.4.5 PID Tuning using GA

The objective of the GA was to minimize the ITAE (Integral of the Time weighted Absolute error) is given as:

$$ITAE = \int_0^{\infty} t|e(t)|\,dt$$

But the GA finds the maximum value of a fitness function. So we used the following fitness function to minimise ITAE:

$$Fitness\ Function = \frac{1}{0.001 + ITAE} = \frac{1}{0.001 + \int_0^\infty t|e(t)|\,dt}$$

3.5 Results

The displacement of the proof mass and the output voltage of the closed loop accelerometer using PID controller tuned using Ziegler Nichols for different step like input acceleration signals are presented in Figure 3.5 and Figure 3.6 respectively. The displacement of the proof mass and the output voltage of the closed loop accelerometer using PID controller tuned using Genetic Algorithm for different step input acceleration signals are presented in Figure 3.7 and Figure 3.8 respectively.

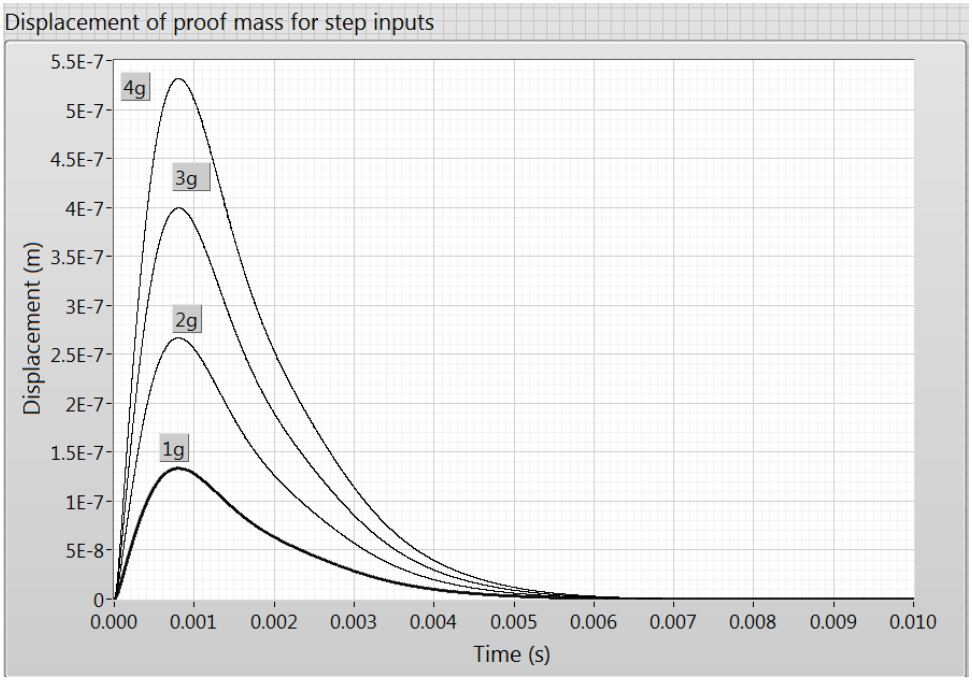

Figure 3.5: Displacement of proof mass for different step inputs.

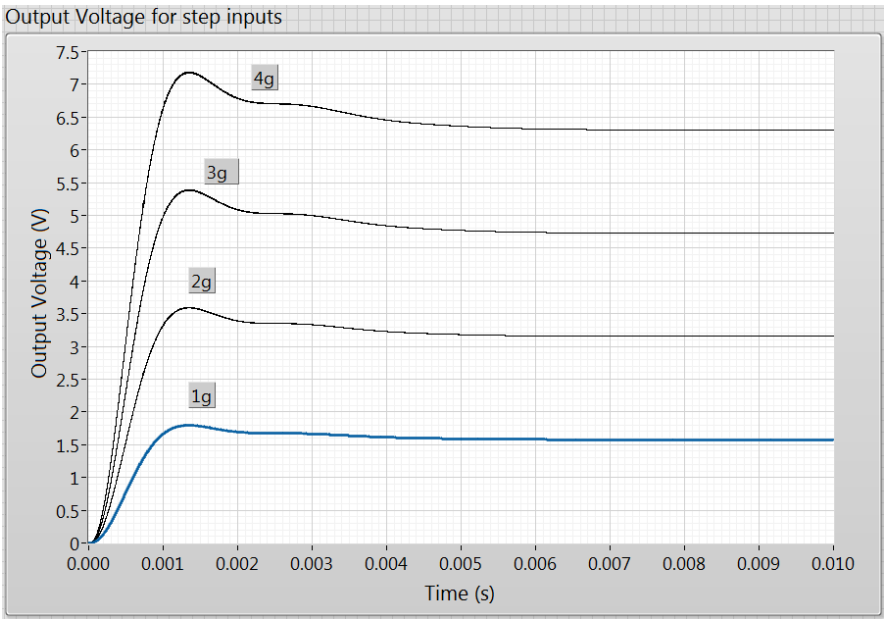

Figure 3.6: Output Voltage of the accelerometer for different step inputs.

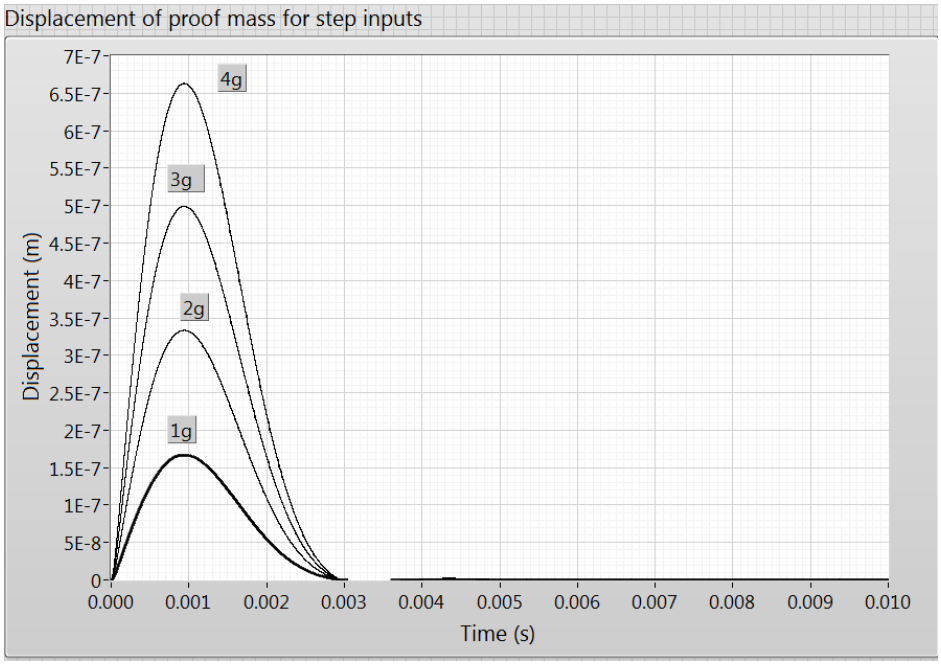

Figure 3.7: Displacement of proof mass for different step inputs.

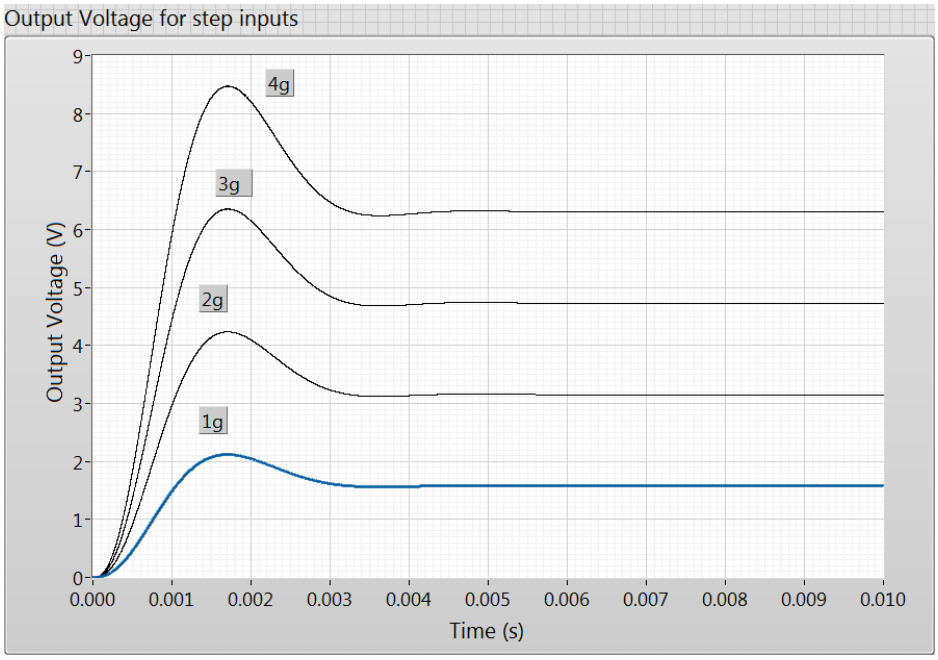

Figure 3.8: Output Voltage of the accelerometer for different step inputs.

***

Chapter Four: **PERFORMANCE ENHANCEMENT OF ACCELEROMETER USING FUZZY LOGIC CONTROLLER**

4.1 Introduction

To further improve the performance of the capacitive MEMS accelerometer in the closed loop method a fuzzy logic controller was designed. The FLC was a Fuzzy PI + Fuzzy PD controller. The tuning was done using GA to minimize the ITAE (Integral of time weighted absolute error).

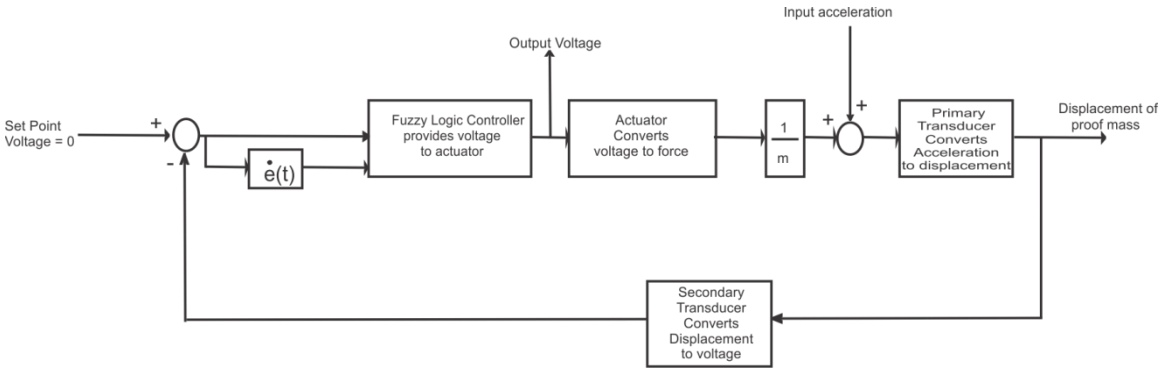

Figure 4.1: Accelerometer and Fuzzy Logic Controller in closed loop.

4.2 Fuzzy Logic

4.2.1 Introduction to Fuzzy Logic

The point of fuzzy logic is to map an input space to an output space and the primary mechanism for doing this is a list of if-then statements called rules. All rules are evaluated in parallel, and the order of the rules is unimportant. The rules themselves are useful because they refer to variables and the objectives that describe those variables. The diagram below provides a roadmap for the fuzzy inference process.

4.2.2 Foundation of Fuzzy Logic

1. **Fuzzy Sets**

   Fuzzy logic starts with the concept of a fuzzy set. A fuzzy set is a set without a crisp, clearly defined boundary. It can contain elements with only a partial degree of membership.

2. **Membership Functions**

   A membership function is a curve that defines how each point in the input space is mapped to a membership value(or degree of membership) between 0 and 1. The input space is sometimes referred to as the universe of discourse. The only condition a membership function must really satisfy is that it must vary between 0 and 1. The function itself can be an arbitrary curve whose shape we can define as a function that suits us from the point of view of simplicity, convenience, speed and efficiency.

4.2.3 Features of Fuzzy Logic

Fuzzy logic has following advantages:

1. Fuzzy Logic is conceptually easy to understand.
2. The mathematical concepts behind fuzzy reasoning are very simple. What makes fuzzy is the 'naturalness' of its approach and not its far-reaching complexity.
3. Fuzzy logic is flexible.
4. With any given system, it is easy to implement it or layer more functionality on top of it without starting again from scratch.
5. Fuzzy logic is tolerant of imprecise data.
6. Everything is imprecise if we look closely enough, but more than that, most things are imprecise even on careful inspection. Fuzzy reasoning builds this understanding into the process rather than tacking it onto the end.
7. Fuzzy logic can model non-linear functions of arbitrary complexity.
8. We can create a fuzzy system to match any set of input-output data. This process is made particularly easy by adaptive techniques like ANFIS(Adaptive Neuro-Fuzzy Inference Systems).
9. Fuzzy logic can be built on top of the experience of experts.
10. In direct contrast to neural networks, which take training data and generate opaque, impenetrable models, fuzzy logic lets you rely on the experience of people who already understand your system.

11. Fuzzy logic can be blended with conventional control techniques.
12. Fuzzy systems don't necessarily replace conventional control methods. In many cases fuzzy systems augment them and simplify their implementations.

4.2.4 Fuzzy Inference system

Information flows from left to right, from two inputs to a single output. The parallel nature of the rules is one of the most important aspects of fuzzy logic systems. Instead of sharp switching modes based on breakpoints, we glide smoothly from regions where the system's behaviour is dominated by either one rule or another.

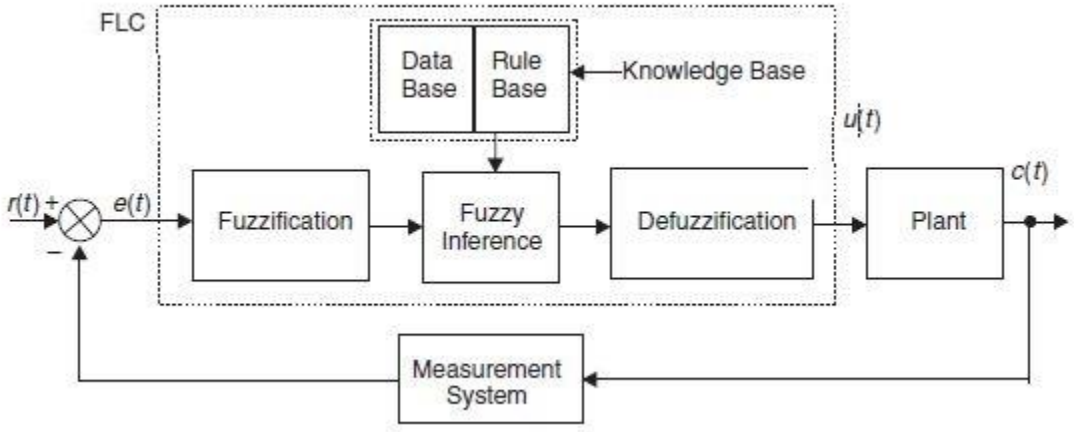

Figure 4.2: Fuzzy logic controller in plant.

There are five parts of fuzzy inference process: fuzzification of input variables, application of the fuzzy operator (AND or OR) in the antecedent, implication from the

antecedent to the consequent, aggregation of the consequents across the rules and defuzzification.

Step1. Fuzzifying Inputs

The first step is to take the inputs and determine the degree to which they belong to each of the appropriate fuzzy sets via membership functions. The input is always a crisp numerical value limited to the universe of discourse of the input variable (in this case the interval between -1 and 1) and the output is a fuzzy degree of membership in the qualifying linguistic set(always the interval between 0 and 1). Fuzzification of the input amounts to either a table lookup or a function evaluation.

Step 2. Apply Fuzzy Operator

Once the inputs have been fuzzified, we know the degree to which each part of the antecedent has been satisfied for each rule. If the antecedent of the given rule has more than one part, the fuzzy logic is applied to obtain one number that represents the result of the antecedent for that rule. This number will then be applied to the output function. The input to the fuzzy operator is two or more membership values from fuzzified input variables. The output is a single truth value.

Step3. Application of the implication method

Before applying the implication method, we must take care of the rule's weight. Every rule has a weight (a number between 0 and 1), which is applied to the number given by the antecedent. Generally this weight is 1(as it is for this example) and so it has no effect at all on the implication process. From time to time we may want to weight one rule relative to the others by changing its weight value to something other than 1.

Once proper weighting has been assigned to each rule, the implication method is implemented. A consequent is a fuzzy set represented by a membership function, which weights appropriately the linguistic characteristics that are attributed to it. The consequent is reshaped using a function associated with the antecedent(a single number). The input for the implication process is a single number given by the antecedent, and the output is a fuzzy set. Implication is implemented for each rule.

Step4. Aggregation of all Outputs

Since decisions are based on the testing of all the rules in an FIS, the rules must be combined in some manner in order to make a decision. Aggregation is the process by which the fuzzy sets that represents the outputs of each rule are combined into a single fuzzy set. Aggregation only occurs once for each output variable, just prior to the fifth and final step, defuzzification. The input of the aggregation process is the list of truncated output functions returned by the implication process for each rule. The output of the aggregation process is one fuzzy set for each output variable. Three methods are

common: max(maximum), prob (probabilistic OR) and sum(simply the sum of each rule's output set).

Step5. Defuzzification

The input for the defuzzification process is a fuzzy set(the aggregate output fuzzy set) and the output is a single number. As much as fuzziness helps the rule evaluation during the intermediate steps, the final desired output for each variable is generally a single number. However, the aggregate of a fuzzy set encompasses a range of output values and so must be defuzzified in order to resolve a single output value from the set.

The most popular defuzzification method is the centroid calculation, which returns the center of area under the curve. There are five built-in methods supported: centroid, bisector, middle of maximum (the average of the maximum value of the output set), largest of maximum and smallest of maximum.

4.3 Fuzzy PI + Fuzzy PD Controller

To implement the Fuzzy PID controller three inputs e (k), Σe(k) and Δe(k) are required. Increasing the number of input variables causes a rise in the dimension of the rule table and, therefore, in the complexity of the system; this makes its implementation more complicated. For this reason, a combination of Fuzzy PI + Fuzzy PD controller was employed instead of three input Fuzzy PID controller.

4.3.1 *Fuzzy PI Controller*

A classical PI controller is described by

$$u_{PI}(t) = K_c\left[e(t) + \frac{1}{T_I}\int e(t)dt\right] \quad [4.1]$$

Differentiating Equation (4.1), the following equation is obtained:

$$\frac{d\,u_{PI}(t)}{dt} = K_c\left[\frac{de(t)}{dt} + \frac{1}{T_I}\,e(t)\right] \quad [4.2]$$

In discrete form, the above equation can be written as:

$$\frac{u_{PI}(k) - u_{PI}(k-1)}{T_s} = K_c\left[\frac{e(k) - e(k-1)}{T_s} + \frac{1}{T_I}\,e(k)\right] \quad [4.3]$$

$$\Delta u_{PI}(k) = K_c\,\Delta e(k) + \frac{K_c}{T_I}e(k) \quad [4.4]$$

where

$$\Delta e(k) = \frac{e(k) - e(k-1)}{T_s}$$

and

$$\Delta u_{PI}(k) = \frac{u_{PI}(k) - u_{PI}(k-1)}{T_s}$$

$$u_{PI}(k) = \frac{K_{UPI}}{1 - z^{-1}}\Delta u_{PI}(k) \quad [4.5]$$

4.3.2 *Fuzzy PD Controller*

A classical PD controller is described by:

$$u_{PD}(t) = K_c\left[e(t) + T_D\frac{de(t)}{dt}\right] \quad [4.6]$$

In discrete form, the above equation can be written as:

$$u_{PD}(k) = K_c \left[e(k) + T_D \frac{e(k) - e(k-1)}{T_s} \right] \quad [4.7]$$

$$u_{PD}(k) = K_c e(k) + K_c T_D \Delta e(k) \quad [4.8]$$

where

$$\Delta e(k) = \frac{e(k) - e(k-1)}{T_s}$$

4.3.3 Fuzzy PI +Fuzzy PD Controller

Finally, the overall Fuzzy PI + Fuzzy PD controller can be obtained by algebraically summing the Equation (4.5) & Equation (4.8)

$$u_{PID}(k) = u_{PI}(k) + u_{PD}(k) \quad [4.9]$$

$$u_{PID}(k) = \frac{K_{UPI}}{1 - z^{-1}} \Delta u_{PI}(k) + u_{PD}(k) \quad [4.10]$$

4.4 Pre-requisites for design of FLC

4.4.1 Fuzzification

Input and output variables of the FLC are usually quantized into sets of classes defined by linguistic labels such as “positive large”, “positive medium”, “positive small”, “zero”, “negative small”, “negative medium”, “negative large”, and so forth. For the experimentation, the inputs and outputs were quantized into 5 fuzzy sets, namely:

PL – Positive Large

PS – Positive Small

ZE – Zero

NS – Negative Small

NL - Negative Large

This quantization was carried out in the range of [-1,1] for inputs as well as output. The membership functions fore(k), Δe(k), $u_{PD}(k) and\ \Delta u_{PI}(k)$ were of triangular type.

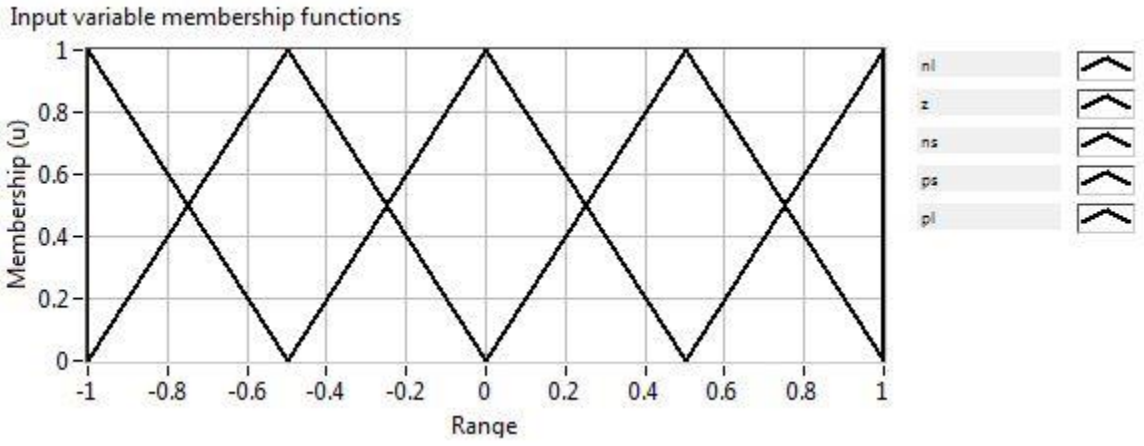

Figure 4.4: Input Variables Membership Functions.

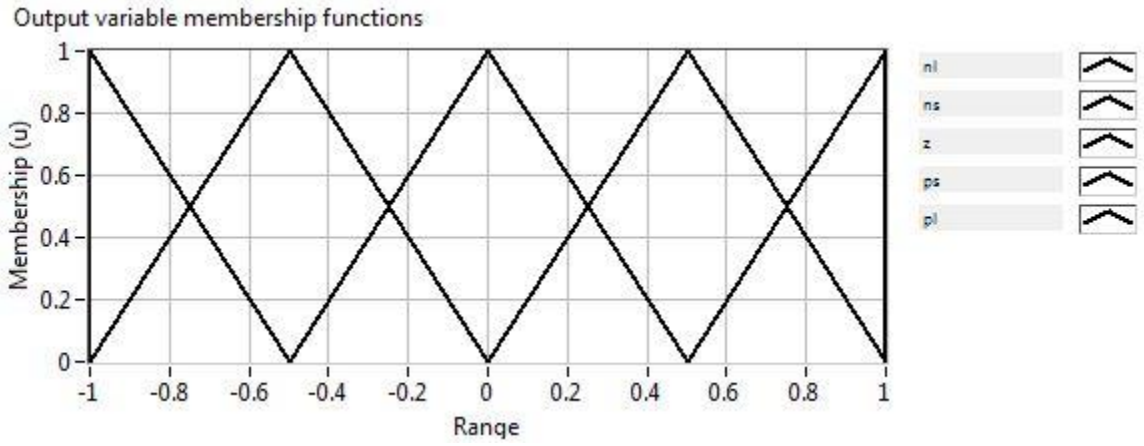

Figure 4.5: Output Variables Membership Functions.

4.4.2 Rule Base

Theoretically, the rule based should be different for Fuzzy PI controller and Fuzzy PD controller but in order to reduce the complexity of design and to increase efficiency, a simple structure of Fuzzy PI + Fuzzy PD controller was used with a single rule base. A PI rule base was considered because PI controller is generally more important for steady state performance.

To define the rules, a Mamdani fuzzy model was chosen. Starting from the inputs' and output's membership functions, a set of nine inference rules were derived for fuzzy PI controller

R1: If e (K) is NL and Δe (k) is NL then Δu (k) is NL.

R2: If e (K) is NL and Δe (k) is NS then Δu (k) is NL.

R3: If e (K) is NL and Δe (k) is ZE then Δu (k) is NL.

R4: If e (K) is NL and Δe (k) is PS then Δu (k) is NS.

R5: If e (K) is NL and Δe (k) is PL then Δu (k) is ZE.

R6: If e (K) is NS and Δe (k) is NL then Δu (k) is NL.

R7: If e (K) is NS and Δe (k) is NS then Δu (k) is NL.

R8: If e (K) is NS and Δe (k) is ZE then Δu (k) is NS.

R9: If e (K) is NS and Δe (k) is PS then Δu (k) is ZE.

R10: If e (K) is NS and Δe (k) is PL then Δu (k) is PS.

R11: If e (K) is ZE and Δe (k) is NL then Δu (k) is NL.

R12: If e (K) is ZE and Δe (k) is NS then Δu (k) is NS.

R13: If e (K) is ZE and Δe (k) is ZE then Δu (k) is ZE.

R14: If e (K) is ZE and Δe (k) is PS then Δu (k) is PS.

R15: If e (K) is ZE and Δe (k) is PL then Δu (k) is PL.

R16: If e (K) is PS and Δe (k) is NL then Δu (k) is PL.

R17: If e (K) is PS and Δe (k) is NS then Δu (k) is ZE.

R18: If e (K) is PS and Δe (k) is ZE then Δu (k) is PS.

R19: If e (K) is PS and Δe (k) is PS then Δu (k) is PL.

R20: If e (K) is PS and Δe (k) is PL then Δu (k) is PL.

R21: If e (K) is PL and Δe (k) is NL then Δu (k) is ZE.

R22: If e (K) is PL and Δe (k) is NS then Δu (k) is PS.

R23: If e (K) is PL and Δe (k) is ZE then Δu (k) is PL.

R24: If e (K) is PL and Δe (k) is PS then Δu (k) is PL.

R25: If e (K) is PL and Δe (k) is PL then Δu (k) is PL.

.

Table 4.1: Rule base for Fuzzy Logic Controller

	Change of error (de)					
		NL	**NS**	**ZE**	**PS**	**PL**
Error (e)	**NL**	NL	NL	NL	NS	ZE
	NS	NL	NL	NS	ZE	PS
	ZE	NL	NS	ZE	PS	PL
	PS	NS	ZE	PS	PL	PL
	PL	ZE	PS	PL	PL	PL

The rule base for this Fuzzy controller can be imagined to be a two dimensional matrix as summarized in Table 4.1. The rows represent the various linguistic values that change of error $\Delta e(k)$, can take and columns indicate the values of error $e(k)$. The entries in this matrix would be the control action that has to be taken described in the linguistic terms.

4.4.3 Fuzzy Inference Engine

The basic function of the fuzzy inference engine is to compute the overall value of the control output variable based on the individual contribution of each rule in the rule base. For the present research work, Mamdani's inference mechanism has been used. The first phase of Mamdani's implication involves min-operation since the antecedent pairs in

the rule structure are connected by a logical 'AND'. All the rules are then aggregated using a max-operation.

4.4.4 Defuzzification

In the present work center of gravity defuzzification method (COG) was used to defuzzify the fuzzy sets into a crisp control signal.

4.4.5 FLC Tuning using GA

The objective of the GA was to minimize the ITAE (Integral of the Time weighted Absolute error) is given as:

$$ITAE = \int_0^\infty t|e(t)|\,dt$$

But the GA finds the maximum value of a fitness function. So we used the following fitness function to minimise ITAE:

$$Fitness\ Function = \frac{1}{0.001 + ITAE} = \frac{1}{0.001 + \int_0^\infty t|e(t)|\,dt}$$

4.5 Results

The displacement of the proof mass and the output voltage of the accelerometer for different step like input acceleration signals are presented in Figure 4.4 and Figure 4.5 respectively.

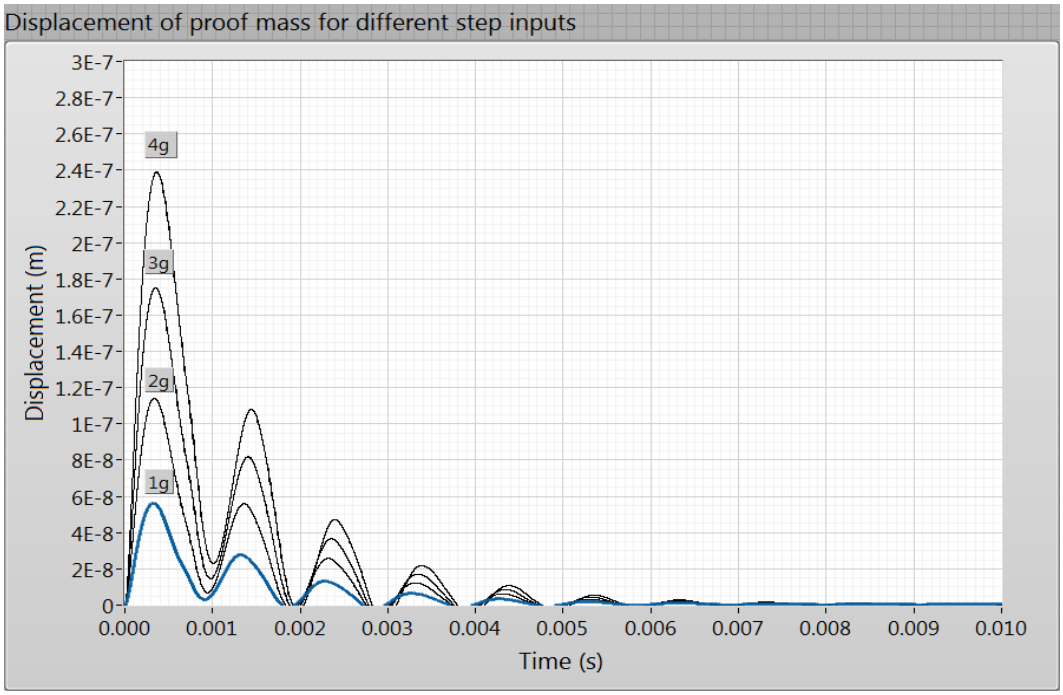

Figure 4.6: Displacement of proof mass for different step inputs.

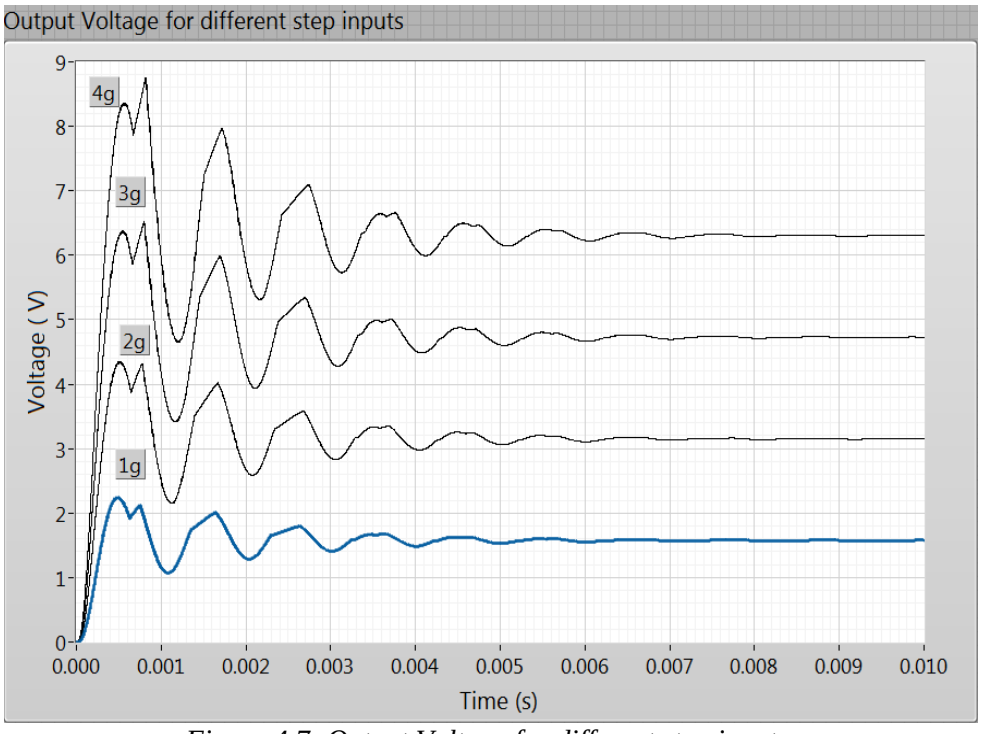

Figure 4.7: Output Voltage for different step inputs.

***

Chapter Five: **CONCLUSION, DISCUSSION AND FUTURE SCOPE**

5.1 Introduction

In this chapter we study comparison between open loop and close loop accelerometer performance on parameters of displacement of proof mass (which defines the linearity range), ITAE (Integral of the Time weighted Absolute error) and output voltage (which give sensitivity of the accelerometer) . In the end the future scope of work is discussed.

5.2 Comparison between open and closed loop performance

5.2.1 Displacement of Proof Mass

The displacement of proof mass is a measure of the linearity range of an accelerometer. The maximum displacement of the proof mass for various configurations is given in Table 5.1. It can be seen that the maximum displacement of proof mass has reduced as the complexity of the system increases, i.e., as we go from open loop to closed loop accelerometer with Fuzzy PI + Fuzzy PD controller tuned using GA. Figure 5.1 is the graphical representation of the comparison between the displacement of proof mass for various configurations.

The following Figure 5.2, Figure 5.3, Figure 5.4 and Figure 5.5 show the linearity range for the different configurations of a capacitive accelerometer. It is seen that the range increases as the complexity of the system increases, i.e. As we go from open loop to closed loop accelerometer with Fuzzy PI + Fuzzy PD controller tuned using GA. The ranges for various configurations are shown in Table 5.2. It is maximum for closed loop accelerometer with Fuzzy PI + Fuzzy PD controller tuned using GA nd minimum for open loop accelerometer.

Table 5.1: Comparison of displacement of proof mass

Input acceleration Here g = 9.8(m/s^2)	Maximum displacement of proof mass (Open Loop Accelerometer) (m)	Maximum displacement of proof mass (Closed loop Accelerometer with PID controller tuned using Ziegler Nichols) (m)	Maximum Displacement of proof mass (Closed loop Accelerometer with PID controller tuned using Genetic Algorithms (m)	Maximum displacement of proof mass (Closed loop Accelerometer with Fuzzy PI + Fuzzy PD controller tuned using Genetic Algorithms) (m)
1g	9.65019E-7	1.33E-07	1.67E-07	5.62E-08
2g	1.93008E-6	2.67E-07	3.35E-07	1.142E-7
3g	2.89522E-6	3.99E-07	5E-07	1.751E-7
4g	3.86052E-6	5.32E-07	6.6E-07	2.389E-7

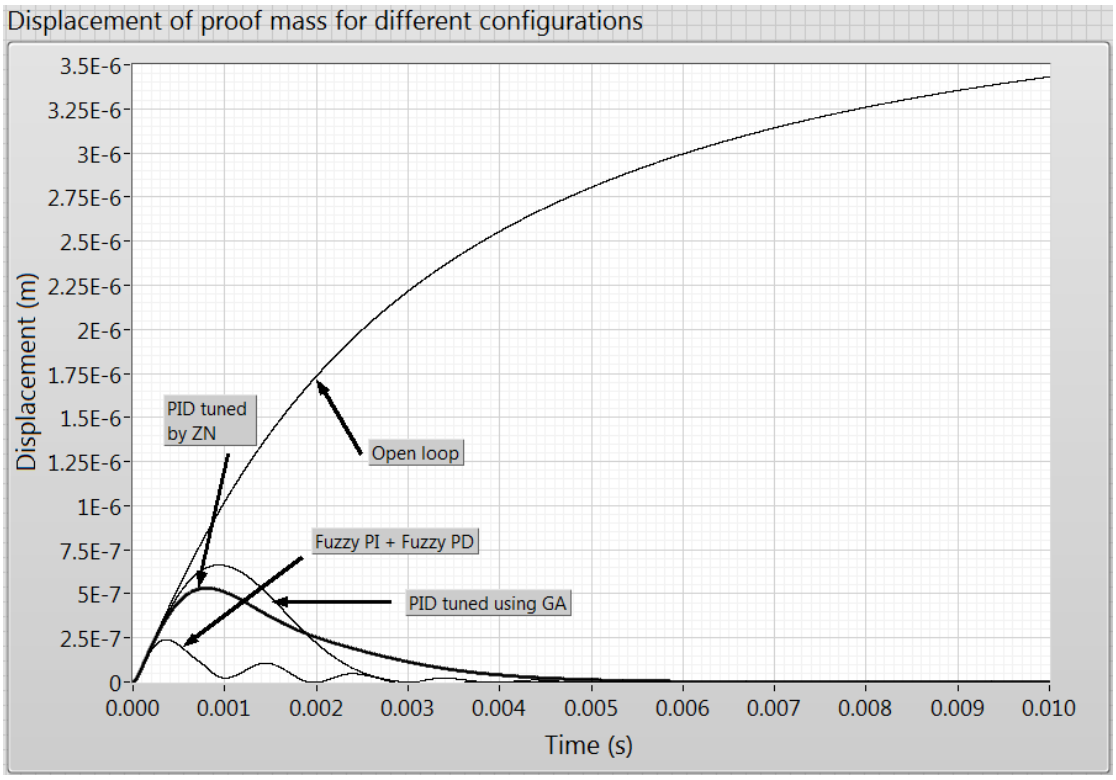

Figure 5.1: Comparative displacement of proof mass for step input of 4g.

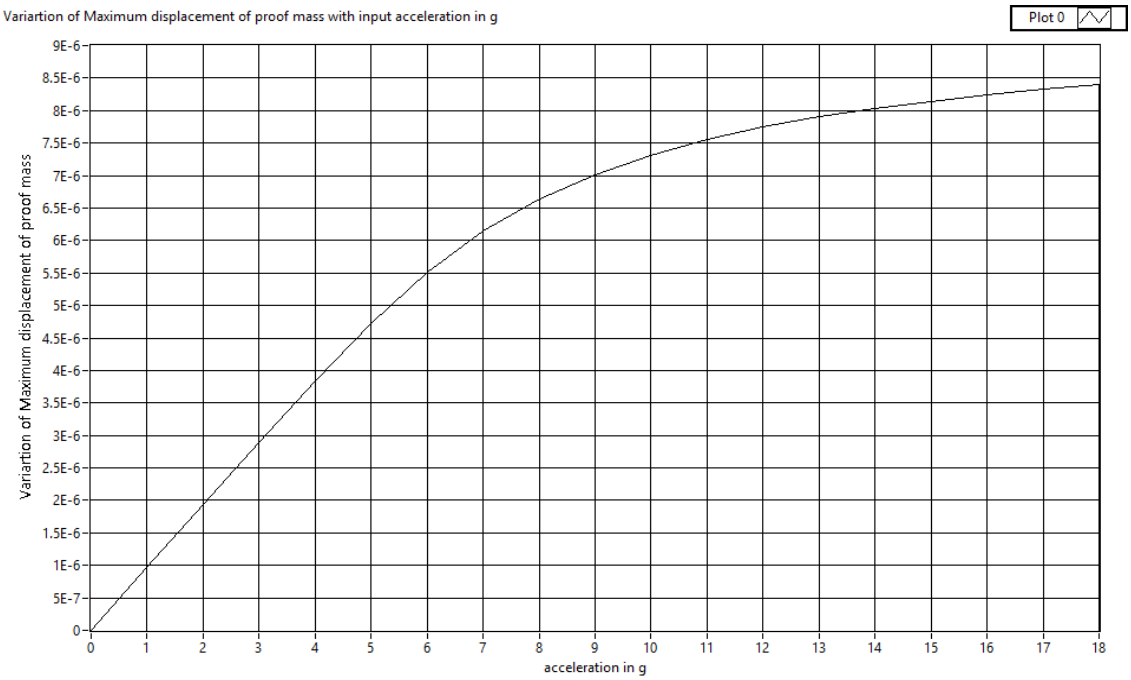

Figure 5.2: Variation of maximum displacement of proof mass for open loop.

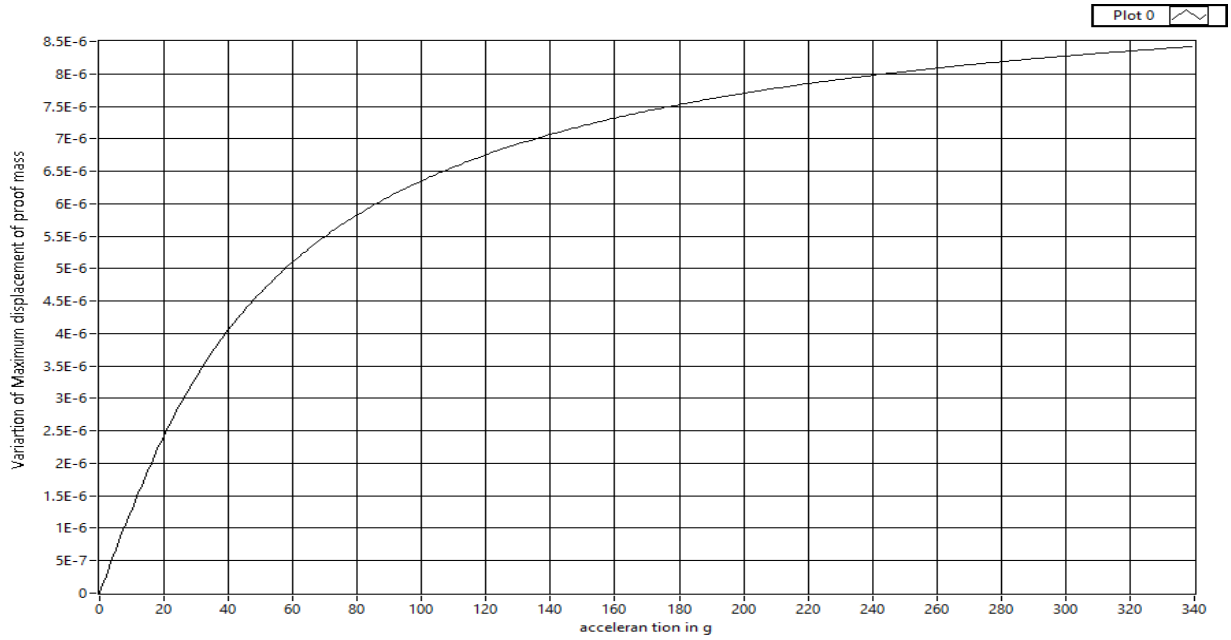

Figure 5.3: Variation of Maximum displacement of proof mass for close loop PID tuned using ZN

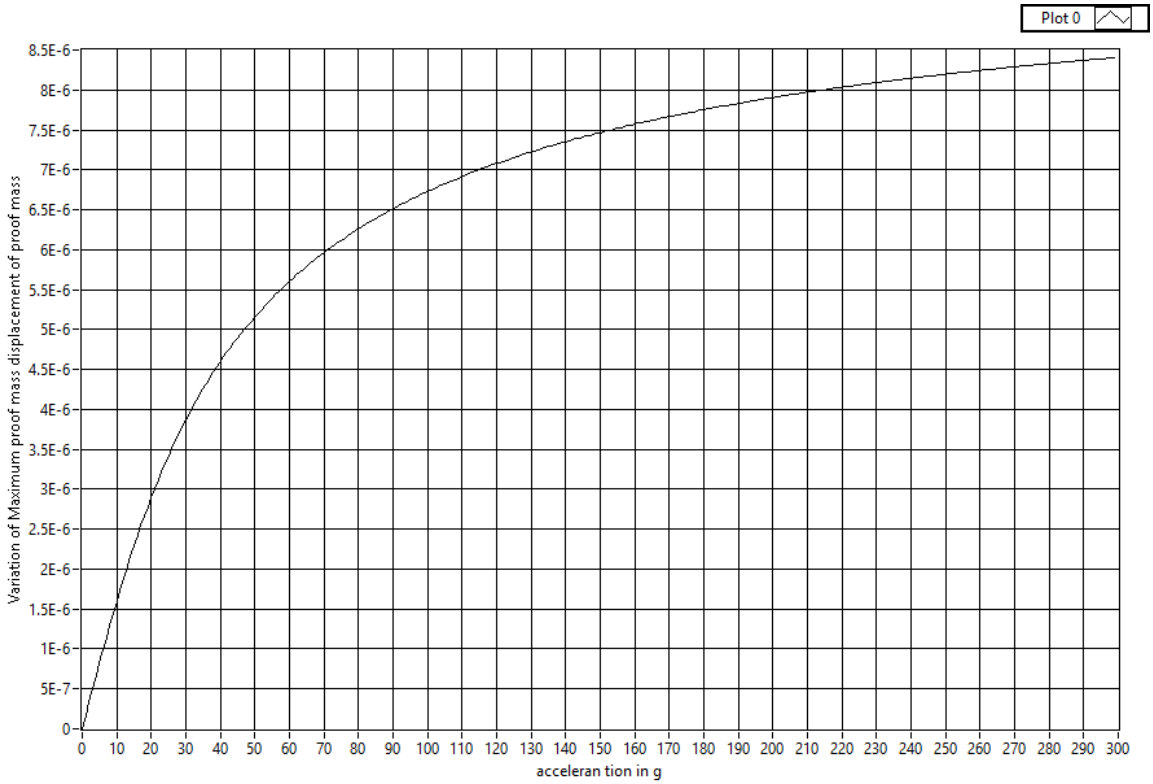

Figure 5.4: Variation of Maximum displacement of proof mass for close loop PID tuned using GA

Table 5.2: Comparison of linear range

Range (Open Loop Accelerometer)	Range (Closed loop Accelerometer with PID controller tuned using Ziegler Nichols)	Range (Closed loop Accelerometer with PID controller tuned using Genetic Algorithms)	Range (Closed loop Accelerometer with Fuzzy PI + Fuzzy PD controller tuned using Genetic Algorithms)
0-4g	*0-20g*	*0-30g*	*0-50g*

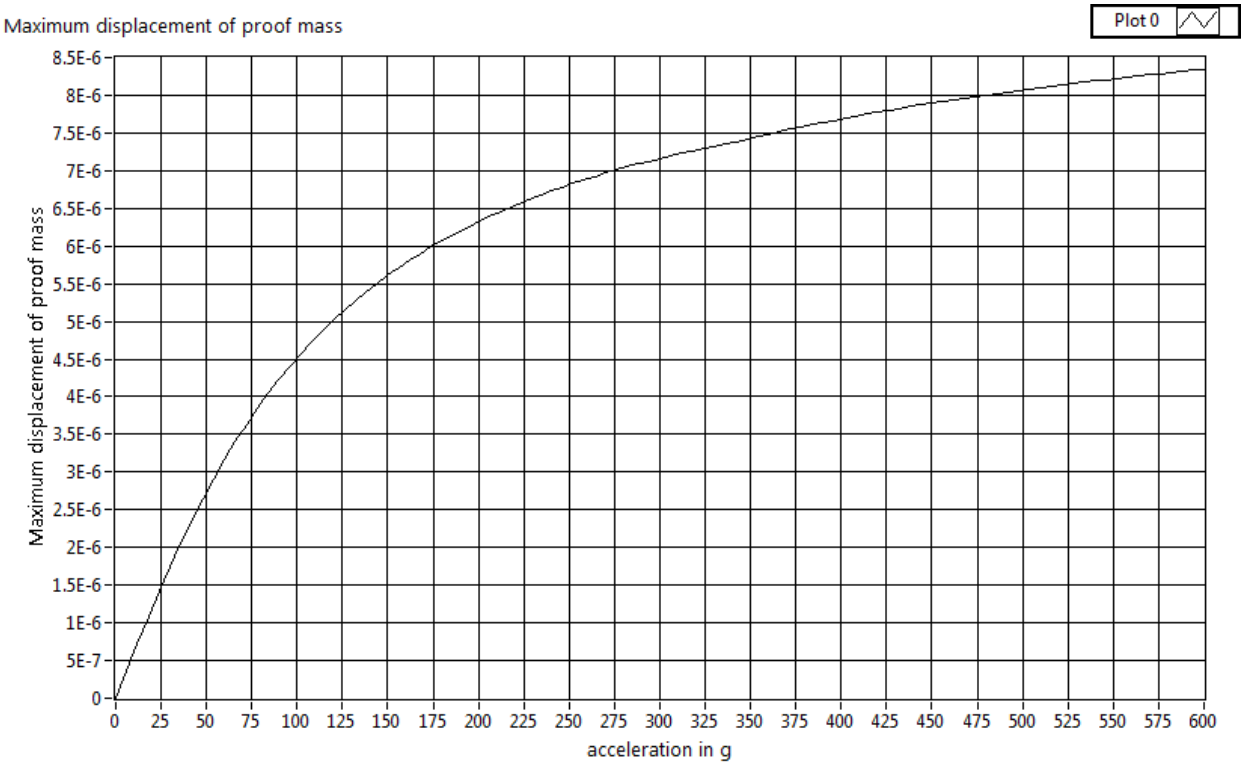

Figure 5.5:Variation of Maximum displacement of proof mass for close loop fuzzy PI +fuzzy PD

5.2.2 ITAE (Integral of the Time Weighted Absolute Error)

The ITAE (Integral of the Time weighted Absolute Error) value calculated for various configurations and is given in Table 5.3. It is seen that the maximum value is for open loop accelerometer and minimum for closed loop accelerometer with Fuzzy PI + Fuzzy PD controller tuned using GA. Basically GAs objective function was to reduce the ITAE and it has reduced the ITAE value by 10 times from closed loop accelerometer with PID controller tuned using Ziegler- Nichols to closed loop accelerometer with Fuzzy PI + Fuzzy PD controller tuned using GA.

Table 5.3: Comparison of ITAE

Input acceleration Here $g = 9.8(m/s^2)$	ITAE (Open Loop Accelerometer)	ITAE (Closed loop Accelerometer with PID controller tuned using Ziegler Nichols)	ITAE (Closed loop Accelerometer with PID controller tuned using Genetic Algorithms)	ITAE (Closed loop Accelerometer with Fuzzy PI + Fuzzy PD controller tuned using Genetic Algorithms)
1g	4.02947E-11	4.00249E-13	2.82255E-13	8.2868E-14
2g	7.92285E-11	8.00323E-13	5.6471E-13	1.52258E-13
3g	1.15564E-10	1.20005E-12	8.47588E-13	2.20598E-13
4g	1.48391E-10	1.59925E-12	1.13115E-12	2.92764E-13

5.2.3 Output Voltage of the Accelerometer

The output voltage of an accelerometer for a given acceleration is a measure of its sensitivity. The larger the output voltage for a given input acceleration the larger is the sensitivity. When the output voltage was calculated and represented in Table 5.4 for various configurations it was seen that it has increased from the open loop accelerometer to the closed loop accelerometer.

Table 5.4: Comparison of Output Voltage

Input acceleration Here g = 9.8 (m/s^2)	Output Voltage (Open Loop Accelerometer) (V)	Output Voltage (Closed loop Accelerometer with PID controller tuned using Ziegler Nichols) (V)	Output Voltage (Closed loop Accelerometer with PID controller tuned using Genetic Algorithms (V)	Output Voltage (Closed loop Accelerometer with Fuzzy PI + Fuzzy PD controller tuned using Genetic Algorithms) (V)
1g	0.450	1.576	1.576	1.577
2g	0.926	3.151	3.151	3.153
3g	1.457	4.727	4.727	4.728
4g	2.078	6.303	6.303	6.303

5.3 Future Scope

We have modeled and simulated a capacitive accelerometer in this thesis. The capacitive accelerometer has a high sensitivity among other accelerometers like

piezoresistive and piezoresistive accelerometer but lower than the tunnelling accelerometer which has an inherent closed loop working. So we can model and simulate the tunnelling accelerometer in the future.

***

REFERENCES

1. Stephen Beeby, Michael Kraft, Graham Ensell, Neil White, "MEMS Mechanical Sensors," Artech House,Inc.,2004,Chapter 8.
2. George Stephanopoulos, "Chemical process control**:** an introduction to theory and practice," PHI Learning Private Limited,2012,Chapter 18.
3. V. Kumar, K.P.S. Rana, Vandna Gupta, "Real-Time Performance Evaluation of a Fuzzy PI + Fuzzy PD Controller for Liquid-Level Process," International Journal on Intelligent Control and Systems,Vol. 13, No. 2, June 2008, pp. 89-96.
4. T.L. Grigorie, "The Matlab/Simulink Modeling and Numerical Simulation of an Analogue Capacitive Micro- Accelerometer Part 1: Open Loop," Proceedings of the MEMSTECH, Ukraine: Polyana, pp. 105-114, 2008.
5. T.L. Grigorie, "The Matlab/Simulink Modeling and Numerical Simulation of an Analogue Capacitive Micro- Accelerometer Part 2: Closed Loop," Proceedings of the MEMSTECH, Ukraine: Polyana, pp. 115-121, 2008.
6. Mitsua Gen, Runewi Chang, "Genetic Algorithm and Engineering Optimization", John Wiley & Sons, Inc., New York, 2000, Chapter 1.

***